OCD Work Unit No. 3212A
USNRDL-TR-1049
29 July 1966

REMOVAL OF SIMULATED FALLOUT FROM ASPHALT STREETS BY FIREHOSING TECHNIQUES

by

L.L.Wiltshire
W.L.Owen

U.S. NAVAL RADIOLOGICAL
DEFENSE LABORATORY

SAN FRANCISCO · CALIFORNIA 94135

ABSTRACT

This report evaluates firehosing as a wet reclamation procedure for the operational recovery of asphalt paved streets contaminated with fallout from a land surface nuclear detonation. Preliminary tests with inert fallout simulant determined the optimum nozzle stream range and firehosing technique. Principal tests, conducted with radio-traced simulants, measured the effects of hosing rate, stream pattern, particle size and mass loading on the fallout removal performance of firehosing.

Several conclusions were indicated: (1) A slow hosing rate (visually controlled) was more effective than a faster rate, regardless of mass loading or particle size range. (2) The removal effectiveness improved with increased particle size range and increased mass loading. (3) An experimental NRDL "flare" nozzle appeared to improve hosing performance at nozzle pressures greater than 150 psi.

Graphs showing the effect of hosing rate, particle size, mass loading and stream pattern on the reclamation performance of firehosing are presented.

SUMMARY

The Problem

Firehosing can be an important procedure for removing fallout during radiological recovery because of its broad application and ready availability. Furthermore, reclamation studies have shown firehosing to be especially effective. Interpretation of test results, however, was limited largely to demonstrating the dependence of removal effectiveness upon fallout mass loadings and firehosing effort, without regard to the effects of fallout particle size range. Since the last firehosing experiments (Stoneman II, 1958), facilities had been developed at the USNRDL Station at Camp Parks to produce simulant in five distinct particle size ranges. Subsequent tests of other methods, sweeping and street flushing, showed removal effectiveness to be a function of particle size range. Therefore it became necessary to investigate this effect on firehosing performance.

Findings

Sand tagged with the radionuclide La^{140} was dispersed at different mass loadings on an asphalt test surface to simulate expected fallout conditions. Two firehosing rates were used, with two types of nozzles, a standard fire nozzle and an experimental NRDL "flare" nozzle, in the removal of different particle size ranges.

It was found that:

1. In most cases, the slow (visually controlled) rate of firehosing removes more material than the fast rate for the same amount of effort.

2. At the slow firehosing rate the hose teams can operate for longer periods of time before tiring.

3. In general, removal effectiveness improves with increased particle size range and increased mass loading. For the expenditure of an effort of 4 nozzle-minutes (12 man-minutes) per 10^3 ft^2, results ranged as follows:

Particle Size Range (μ)	Nominal Mass Loading (g/ft^2)	Removal Effectiveness (Residual Fraction)
44 - 88	4.0	0.16
	24.0	0.07
350 - 700	4.0	0.005
	24.0	0.003

4. The effects of stream pattern were not completely established. It is quite possible that hosing performance can be improved through use of the flare nozzle, if the nozzle pressure is kept at 150 psi or greater.

CONTENTS

FIGURES (Cont'd)

GLOSSARY

Countermeasure. Any of several methods or principles used in reducing the effects of fallout. Two types of countermeasures are reclamation and radiation shielding.

Effectiveness. A measure of the fallout reduction capability of a given countermeasure or an entire recovery operation. It is expressed as the residual fraction of either the decay-corrected original radiation level or the amount (mass) of fallout material initially present.

Pass. One complete coverage of a target component by a reclamation method. Where two or more methods are sequentially applied, such as a sweeping pass followed by a firehosing pass, this combined sequence of coverage is referred to as a cycle.

Reclamation. The reduction of radiation intensity by either removing fallout material from a sensitive area or covering it in place by mixing or burial.

Removal. A specific form of reclamation wherein the fallout material is dislodged and transported from the originally contaminated area, as in the case of firehosing.

Standard Intensity.* The hypothetical, unshielded radiation intensity that would be observed (three feet above an infinite smooth plane) one hour after burst if all the fallout were deposited by that time.

Stream Range. The distance between the nozzle and the point of stream impact.

Stream Pattern. The shape of the water stream leaving the nozzle.

Visually Controlled Firehosing Rate. The rate at which the fallout is seen to be moved ahead by the water stream.

---

*Standard Intensity is defined also in "Terminology for Fallout Studies," a paper prepared by The Postattack Division, Office of Civil Defense, to unify the terminology in all fallout studies.

CHAPTER I

INTRODUCTION

Throughout the develop nt of radiological countermeasures, firehosing has been considered an important fallout removal method. The equipment required for its implementation is universally available. The technique of firehosing is straightforward and requires no great skill. Firehosing is extremely flexible, since it can be applied to areas not accessible to other known methods. Finally firehosing has been shown to be an effective removal method by prooftests on both simulated and actual fallout.

1.1 HISTORY AND BACKGROUND

Firehosing was the first method employed in the removal of fallout, at Operation Crossroads in 1947. Since the ionic type of fallout from the underwater detonation was very tenacious, firehosing removed only about 50 % of the fallout from the contaminated naval vessels. In later tests at Operations Castle and Redwing, firehosing achieved a similar degree of fallout removal on shipboard surfaces.

Firehosing was first used to remove mass quantities of particulate fallout simulant in the 1956 Stoneman I Operation.[1] Solid particulate fallout was simulated by tagging batches of local soil with La^{140} and then dispersing it on roofs and paved areas. Firehosing was 95 % effective in removing this type of fallout simulant. Similar tests were conducted again in the 1958 Stoneman II Operation.[2] Here the effects of operational variables and environmental factors upon

firehosing performance were observed. Firehosing achieved the same degree of removal as that at Stoneman I, but with significantly less effort because of improvements in hosing technique.

The completion of the Stoneman Operations coincided with the development of a theoretical cleaning equation which described the basic fallout removal process. This theoretical concept was used to evaluate the Stoneman II firehosing data. From this an empirical formula* was derived that provided an approximate fit to the firehosing data. The resultant curves showed the decrease in residual mass of fallout material as a function of firehosing effort expended.

After the Stoneman Operations a fallout model was developed by Miller[3] which related pertinent fallout characteristics to known nuclear detonation conditions. In particular, the model revealed that for certain combinations of weapon yields and downwind distances, high standard intensities are possible with considerably less concentration of fallout material (g/ft^2) than had been previously believed. At the same time, the fallout model gives the particle size range for each predicted mass loading. Means for producing fallout simulant in these particle size ranges were developed.

All subsequent NRDL investigations of reclamation methods have been planned from criteria dictated by Miller's model. Until the experiment presented in this report, firehosing tests had not included this new approach. However, the somewhat analogous street flusher tests of Clark and Cobbin[4] indicated that the reclamation performance of wet methods was dependent upon particle size. Since no confirming inferences could be drawn from Stoneman II results, it became mandatory to reinvestigate firehosing in this new light.

---

*See Section 4.4 for details.

1.2 OBJECTIVES

The ultimate objective of this experiment was to establish optimum firehosing performance characteristics by observing the interaction between removal effectiveness and those factors affecting operational efficiency.

Specific objectives in support of the above were as follows:

1. To determine and measure equipment variables governing firehosing performance.

2. To establish (within practical manpower limits) the most efficient firehosing technique.

3. Under the optimum combination of operational variables found in 1 and 2 above, to measure firehosing performance in terms of removal effectiveness and required effort.

All three objectives were investigated for a limited selection of fallout mass loadings and particle size ranges.

1.3 EXPERIMENTAL APPROACH

The experiment was performed in two major stages, preliminary and principal. The preliminary stage involved 19 tests conducted with inert (non-radioactive) sand simulant. These tests met the first two objectives by resolving the operational factor of stream range and hosing technique. These findings were standardized into an optimum firehosing procedure that was followed for the remainder of the experiment. The principal stage consisted of 29 tests performed on simulant tagged with radioactive isotope. These tests met the last objective by observing the effects of cleaning rate, particle size, mass loading and stream pattern on firehosing effectiveness.

Of the 29 principal tests listed in Table 1.1, 24 employed a conventional 5/8-in. fire nozzle. Of these, two tests were conducted for each of 12 simulated fallout conditions. In each case, one of the two was conducted at a slow (visually controlled)* firehosing rate of 400 to 600 ft^2/min. The remaining 5 tests employed an NRDL experimental "flare" nozzle. These tests were conducted at the visual rate only. All tests were performed on asphalt surfaces.

The 12 simulated radiological conditions were defined by particle size ranges (PSR) of 44-88 μ, 88-177 μ, 177-350 μ and 350-700 μ; and by mass loadings of 4, 12, 24, 50 and 100 g/ft^2. For complete radiological conditions including weapon yield, standard intensity, distance from ground zero, as well as PSR and mass loading, see Appendix B, Table B.1.

TABLE 1.1

Scheme of Principal Reclamation Tests

Nominal Mass Loading (g/ft^2)	Particle Size Range (Code Letter and Particle Diameter in Microns) A 44-88	B 88-177	C 177-350	D 350-700
	Fire Nozzle; 5/8 in. Diameter Orifice			
4	2[a]	2	2	2
12			2	
24	2	2	2	2
50		2	2	
100		2		
	Flare Nozzle; 3/8 by 9/16 in. Elliptical Orifice			
24	1	1	2	1

a. Entries indicate number of tests conducted for each mass loading and PSR shown.

Note: See Table B.1 for a complete description of the simulated radiological conditions.

*See Glossary.

CHAPTER II

FUNDAMENTALS OF FIREHOSING

2.1 THE REMOVAL PROCESS

Solid particulate fallout, typical of land surface explosions, is held to target surfaces chiefly by the force of gravity. It is the task of removal methods to physically lift these particles off a surface and carry them away or move them along the surface. Firehosing methods use the energy of high pressure water streams to achieve this removal action. The force of the fluid jet impinging upon a contaminated surface dislodges and displaces particles from their original rest position. Soon the particles are redeposited by the spent runoff water at a new position downstream. The transport of a mass of particles to a collection point or disposal site requires that this process be repeated over and over as the nozzle and stream advance upon a contaminated area.

The water that imparts initial acceleration to particles at stream impact will carry them some distance downstream to new rest positions. This distance can be significantly increased if an adequate water flow rate can be established at the surface in the area beyond the stream impact region. Good drainage, high nozzle pressures, and proper hosing technique tend to improve flow conditions.

2.2 GOVERNING FACTORS

A number of factors are known to govern the effectiveness of the firehosing removal process. These have been classified as being either environmental or operational.

Environmental factors are considered to be outside the control of recovery personnel. There are three sub-categories:

a. Terrain factors - surface characteristics (composition, finish and condition) and drainage features (slope, crown, gutters, catch basins, etc.)

b. Fallout properties - mass loading, particle size range, and distribution.

c. Climatic conditions - as found in temperate regions compared with colder climates, where the conditions are complicated by snow and ice.

Operational factors are more readily controlled and, within reasonable limits, may be adjusted toward improving firehosing performance. These factors also are of three sub-categories:

a. Energy of fluid streams - expressed by hydrodynamic properties such as pressure, velocity, and flow rate (see Ref. 2).

b. Control of fluid streams - shaping and directing the stream through proper nozzle design and nozzle attitude.

c. Operational performance - evidenced in the hosing technique, forward progress (or rate), required effort (equipment-hours or man-hours) and water consumption rate; and influenced by condition of equipment, addition of towing devices, and the adverse effect of human fatigue.

It will not be the purpose of this report to analyse all these factors in detail. As indicated in Section 1.3, observations will be made of the effects of factors found in environmental category b and operational categories b and c. Information on the remaining categories is available in References 3, 4 and 5.

2.3 OPERATIONAL PRINCIPLES

From all the past firehosing experiments on both actual and simulated fallout, certain operational principles have been found to always hold. These principles, described below, represent the common sense solutions of the equipment-handling problems confronting firehosing teams. In additions, when put into practice, these principles lead to improved reclamation effectiveness.

2.3.1 Job Description

For a single nozzle and hose combination, a firehosing team consists of three men: nozzleman, backup man, and hoseman. The latter two must work closely with the nozzleman, since he is in control. The nozzleman not only directs the water stream but he matches the team's progress with the apparent (visual) fallout removal rate. The backup man absorbs most of the nozzle thrust so as to prevent the nozzleman's being pushed off balance by hose side-whip. He does this by firmly supporting the hose and keeping it aligned straight behind the nozzleman at all times. This allows the nozzleman to concentrate on moving the fallout. The hoseman relieves the other men of having to drag the hose. He also keeps it free of kinks and clear of obstructions.

2.3.2 Hosing Technique

After the team starts hosing, a distance of approximately 25 feet is maintained between the nozzle and the point where the stream impacts upon the contaminated area. With the nozzle at a comfortable height (approximately 40 in. in these tests), the nozzle man plays the impinging water stream back and forth across the receding fallout as it is washed along the surface. By making use of the natural drainage, the stream is directed so as to push the fallout material to convenient collection points down slope. For streets this means

taking advantage of the longitudinal slope and crown to wash the fallout from centerline to gutters to drainage openings. The progress of the firehosing operation is controlled visually to match the rate at which the fallout moves ahead of the water stream.

2.3.3 Equipment Selection

Because of its flexibility and lighter weight, the 1-1/2 in. firehose has proved ideal for reclamation work. Aside from delivering water from distant hydrants, the larger (2-1/2 or 3 in.) diameter hoses are definitely not recommended for firehosing. Their greater weight and nozzle thrust (due to higher flow rates) increase the manpower requirements to six men without any attendant increase in removal effectiveness.

Nozzles most commonly available for 1-1/2 in. hoses have either 1/2-in. or 5/8-in. orifices. It has been found that men can work with either for extended periods of time if the nozzle back thrust is less than 50 pounds. For this reason the nozzle pressure should be kept between 75 and 80 psi for 5/8-in. orifices and between 115 and 120 psi for 1/2-in. orifices.

2.3.4 Precautionary Measures

It must be stressed that these high pressure hose and nozzle combinations are very dangerous tools. Under no condition should the water pressure be applied to an unattended hose or nozzle; nor should the existing pressure be increased without the nozzleman's expressed permission.

2.3.5 Waste Disposal

Under ideal conditions it will be possible to flush accumulations of fallout material through curb inlets into storm drains and sewers. In the case where drains are spaced so far apart that the mass build-up of fallout ahead of the water stream becomes excessive, firehosing will be inadequate to the task of waste disposal. For such situations,

it will be necessary to leave periodic deposits of fallout along the street. These deposits will be picked up later by disposal crews manning shovels, end-loaders and trucks.

This procedure was carried out in a subsequent firehosing experiment.* An asphalt street measuring 32 ft by 280 ft was contaminated with a simulant mass loading of about 100 g/ft^2. Two firehosing teams were able to progress 140 ft before having to leave a windrow and move on. This windrow and the one collected at the terminal end of the test street each weighed about 1000 lb.

It took over 17 min for a two man team** to shovel these deposits into an end-loader for removal to the dump. By comparison, the firehosing phase took only 14-1/2 min. However, firehosing required five men while only 2 to 3 men (including driver) were involved in waste disposal. Because of the increased radiation exposure, waste disposal operations may require far more manpower than firehosing itself.

2.4 PRELIMINARY-TEST FINDINGS

As described in Section 1.3, these preliminary tests measured the equipment and procedural variables which contributed most toward improved firehosing performance. In addition, this operational information was useful in saving time, expense and dosage to test personnel during the principal tests. The preliminary tests were conducted with inert sand using the same PSRs as the principal tests.

---

* Test results were obtained at Camp Parks in 1964. The report is in preparation.

**One and usually two men were shovelling during the disposal operation. Due to the difficulty in positioning the end loader with respect to simulant deposits and curbs, it was not always possible for both men to work simultaneously.

Two phases of preliminary tests were conducted, giving the results described in Appendix A. The first phase established the limits (in feet) of the optimum stream range* for each PSR as follows:

Particle Size Range (μ):		44-88	88-177	177-350	350-700	700-1400
Optimum Stream Range	Upper Limit:	21	25	26	28	28
	Lower Limit:	16	19	21	24	24

These ranges proved to be readily attainable for operational situations.

Using the above stream range information as a guide, a second phase of tests was conducted to establish the most efficient firehosing technique. A comparison of three different approaches showed that the technique developed at the Stoneman II Operation was the most efficient. This is the technique described in Section 2.3.2, and it was used throughout all the principal tests discussed later, in Chapters III and IV.

*See Glossary.

CHAPTER III

PREPARATIONS FOR CONDUCT OF THE PRINCIPAL TESTS

3.1 TEST SITE

The principal tests were conducted on the test strip in Camp Parks used previously for the evaluation of a motorized street flusher.[4] Because of the many features incorporated into the design for the flusher tests, this facility was especially suited to the firehosing test. These features are shown in Fig. 3.1.

The paved test strip is 140 ft long and 31 ft wide. One half of the strip is paved with concrete and the other with asphalt. The firehosing performance tests were confined to a 95 ft section of the asphalt half, between the two curb inlet gratings.

Eighteen-inch concrete gutter aprons and 8-in. curbs line each side of the test strip. A drainage trench surrounds the test strip and street gratings permit vehicular traffic. A sump in the southwest corner section collects run-off water until it is pumped to a distant holding basin. The sump also is used to collect displaced simulant on screens for quick transfer to the waste disposal pit. The drainage trench and sump system, being deep, provide shielded locations for the displaced simulant. This shielding reduces the dosage received by test personnel. It also minimizes the contribution of stray radiation when the activity on the test surface is measured.

The test area was large enough to establish average radiation values under simulated operational firehosing procedures, and it was small enough to ensure economical use of material and manpower.

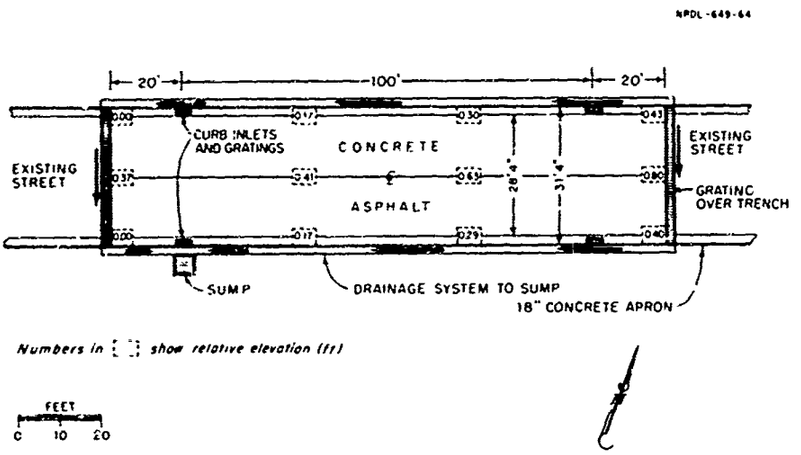

Fig. 3.1 Plan of Test Area

3.2 DESCRIPTION OF FIREHOSING EQUIPMENT

The firehosing team manned a 1-1/2-in. firehose delivering water through a standard tapered nozzle (Fig. 3.2). To maintain a constant pressure at the nozzle, a 500-gpm fire pump (Fig. 3.3) was inserted into the system at the fire hydrant. A 2-1/2-in. firehose delivered the water to the 1-1/2-in. fire hose at the test area. A wye-gate inserted between the 2-1/2 and 1-1/2-in. firehoses provided a safety control close to the crew. Adjustment of the wye-gate by-pass valve attained the desired nozzle pressure, while allowing the pump to run unattended at a constant pressure.

Two nozzles were used in the experiment. A standard tapered fire nozzle with the 5/8-in. orifice was selected over one with the 1/2-in. orifice nozzle, for reasons given at the end of Section A.1 of the Appendix. A standard nozzle gives a slender cone-shaped stream of water at working pressure of 75 to 80 psi. Later in the experiment a special flare nozzle was introduced. It has a 3/8-by-9/16-in. elliptical orifice which delivers a flat fan-shaped stream of water at working pressures of 120 to 160 psi. It is easy to manipulate and acts like a water broom. The flare nozzle is shown in Fig. 3.4. The following table summarizes the hydrodynamic variables characterizing each nozzle as employed in these tests.

Nozzle Type	Orifice Diam. (in)	Nozzle Press. (psi)	Nozzle Thrust (lb)	Flow Rate (gpm)
Std. Fire Nozzle	5/8	75	46	100
Std. Fire Nozzle	1/2	117	46	80
NRDL Flare Nozzle	3/8 x 9/16	120	36	60
NRDL Flare Nozzle	3/8 x 9/16	160	46	70

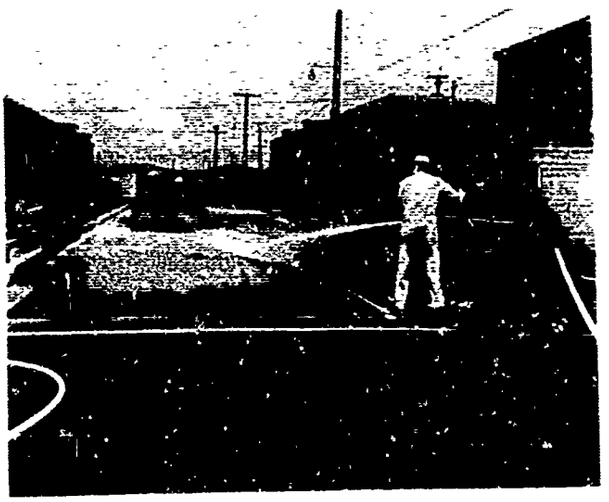

Fig. 3.2 Typical firehosing test run for removal of simulant from left half of street.

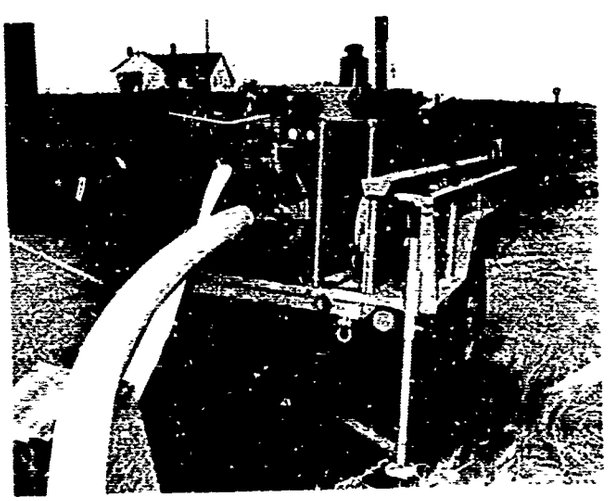

Fig. 3.3 500-gpm, Trailer-Mounted Fire Pump for boosting hydrant pressure.

NRDL 649-64

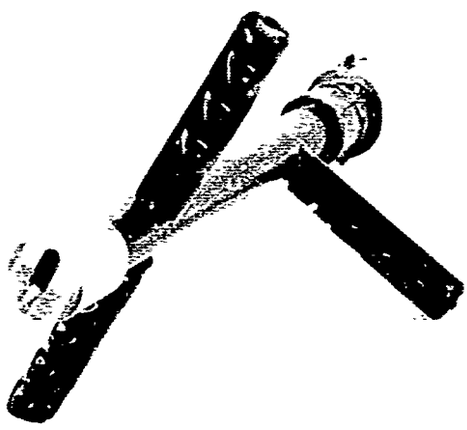

Fig. 3.4 USNRDL Flare Nozzle, With Elliptical Orifice Visible.

3.3 SIMULANT PRODUCTION CONTROL

Facilities for producing fallout simulant were available at Camp Parks, having been developed for previous reclamation projects. The production of fallout simulant consisted of the following phases: isotope selection, hot-cell processing of the isotope,[5] sieving of the bulk carrier material (commercial sand) into particle size ranges, tagging and coating the bulk carrier material, and analyzing the resulting fallout simulant. A complete description of this multi-phase operation is given in Refs. 4 and 5. It should be mentioned here that tests were made on simulant samples from all batches produced, to determine the loss of activity due to leaching by water action during firehosing.* This loss was found to be usually less than 0.1 %.

3.4 DISPERSAL OF FALLOUT SIMULANT

One of the test conditions was a uniformly dispersed initial mass of simulant on the test area. The mass loading (g/ft^2) was dictated by the fallout environment being simulated for that particular test (see Tables 1.1 and B.1). Uniform mass loadings were achieved by dispersing the simulant over a known area by means of a calibrated, hand operated lawn spreader (see Fig. 2.7, Ref. 4). The average initial mass loadings were measured by weighing the spreader before and after dispersal.

3.5 RADIATION INSTRUMENTS

A mobile, shielded and collimated gamma detector was used to measure the directional radiation response at the numbered points

*For a description of the routine leach test procedure - see Appendix I of Ref. 6.

indicated in Fig. 3.5. The trailer mounted assembly includes power supply, collimated detector head and enclosed counter electronics and print-out machine (see Fig. 2.9, Ref. 4). This field instrument employs a sodium iodide scintillation crystal, coupled to a photomultiplier tube within a thick lead shield. The detector's physical characteristics are:

1. The crystal is 1 in. in diameter and 1 in. thick.
2. It is approximately 23.5 in. above the ground.
3. Its lead shield is 6 in. thick.
4. It has an aperture diameter of 2-7/16 in.
5. Its field of view is defined by a cone having an included angle of approximately 110°.

A survey instrument or radiac was used to measure the general area radiation levels at the lettered points indicated in Fig. 3.5. It was also used to monitor personnel and equipment. This radiac, an AN/PDR 27-C radiation detector and indicator, is portable, water-tight and battery-operated.

A 4-pi ionization chamber, a stationary laboratory instrument (Fig. 2.8, Ref. 4), was used for fallout simulant assay, decay, and leach measurements of fallout simulant. It is a well-type, high-pressure ionization chamber, surrounded by a 3-in. lead shield and filled with argon gas to a pressure of 600 psi. An axial well allows introduction of the sample to the approximate center of the sensitive volume of the chamber. This gives a measured geometry of approximately 4-pi steradians. The chamber current is amplified and read on a meter.

3.6 TEST PROCEDURES

3.6.1 Firehosing Procedures

This section contains the operational procedures for the principal tests only (those employing radioactive tracer). Details of the preliminary test procedures are given in Appendix A.

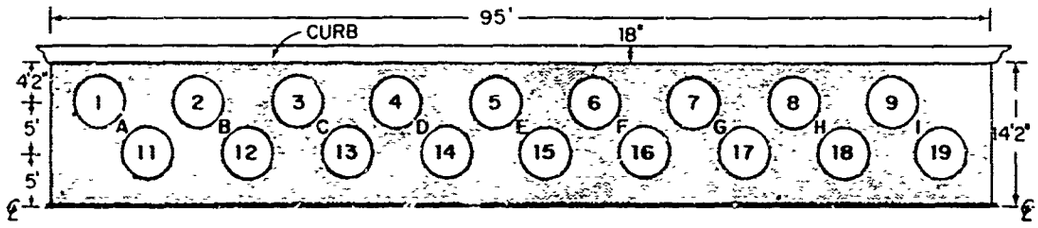

Fig. 3.5 Counting Stations on Asphalt Test Ship

Every firehosing test was conducted in accordance with the principles described in Section 2.3. The firehosing procedure always started at the same end of the test surface and finished at the other end. Such a coverage comprised one pass. Visually controlled (slow rate) tests required two passes. Fast rate tests, conducted at approximately twice the visual rate*, required at least 3 and usually 4 passes.

A typical test run was carried out in the following sequence. The asphalt test area and drainage trench were thoroughly flushed of all residue to lower the residual background radiation level from previous tests. The background was then measured with the shielded detector and with the radiac (see 3.6.2). Fallout simulant at a known mass loading and PSR was dispersed over the test area, and the initial radiation measurements were made with both instruments. The firehosing operation was performed as described above. Next the residual radiation was measured with both instruments. Radiation measurements were made after each additional firehosing pass.

A principal test consisting of two firehosing passes required approximately 6 hr, of which 20 % was devoted to hosing and 80 % to instrumentation and data collection.

3.6.2 Instrument Procedures

The shielded gamma detector was calibrated with a Co^{60} standard at a preselected point one block (approximately 300 ft) from the test area. This eliminated any radiation contributions from the test area. Background counts were made only at odd-numbered stations, but the initial and subsequent radiation measurements were made at all the numbered stations (Fig. 3.5).

The radiac was also calibrated one block (approximately 300 ft) from the test area with the Co^{60} standard. A radiac survey was then taken at only the lettered stations (Fig. 3.5).

*Two distinctly different rates were employed to determine whether the anticipated loss in removal effectiveness at the faster rate would be justified by significant savings in the applied time (and exposure) of the firehosing team.

CHAPTER IV

RESULTS AND DISCUSSION

4.1 PRESENTATION OF RESULTS

The cleaning performance (principal) test results are presented in Tables 4.1 and 4.2 (for raw data see Appendix D). The values in Table 4.1 have been reduced from the shielded gamma detector surveys and include results from the 5/8-in. fire nozzle only. Table 4.2 compares the results of the 5/8-in. fire nozzle with those of the special flare nozzle, as determined from limited radiac surveys.

Tables 4.1 and 4.2 contain the same type of data for each particle size range. The nominal mass loading represents the desired simulant concentration derived in Appendix B. The average initial mass ($\overline{M}_o$) is the actual concentration achieved on the test area, as determined by weight. The pass numbers indicate how many cleaning passes were made during a given test. The cleaning rate (R) includes both slow and fast rate data.

The average residual mass ($\overline{M}$) and average residual fraction ($\overline{F}$) for each cleaning pass were determined from Equations 4.1 and 4.2. The radiation measurements from Appendix E were converted to mass units before being entered in Tables 4.1 and 4.2. This conversion is based on the proportional relationships:

$$\overline{M} = \overline{M}_o \ (\overline{I}/\overline{I}_o) \qquad (4.1)$$

TABLE 4.1

Cleaning Performance Test Results For 5/8 in. Fire Nozzle*

Nominal Mass Loading (g/ft^2)	Average Initial Mass $\bar{M}_o$ (g/ft^2)	Pass No.	Cleaning Rate, R (ft^2/min)	Average Residual Mass $\bar{M}$ (g/ft^2)	Cumulative Effort E $\frac{(Noz\ Min)}{(10^3\ ft^2)}$	Average Residual Fraction $\bar{F}$
			PSR: (A) 44-88 μ			
4.0	4.26	1	443	0.88	2.26	0.21
		2	543	0.66	4.00	0.16
4.0	4.43	1	739	0.98	1.35	0.22
		2	831	0.72	2.56	0.16
		3	950	0.64	3.61	0.14
24.0	24.04	1	459	2.04	2.18	0.085
		2	475	1.54	4.28	0.064
24.0	24.10	1	760	7.81	1.32	0.32
		2	893	6.73	2.44	0.28
		3	887	6.13	3.56	0.25
		4	887	6.01	4.69	0.25
			PSR: (B) 88-177 μ			
4.0	3.76	1	484	0.63	2.07	0.17
		2	559	0.30	3.86	0.11
4.0	3.76	1	985	2.42	1.01	0.64
		2	1,008	1.65	2.01	0.44
		3	937	1.09	3.07	0.29
		4	930	0.84	4.15	0.22
24.0	24.2	1	418	0.56	2.39	0.023
		2	456	0.34	4.41	0.014
24.0	24.4	1	782	4.73	1.28	0.19
		2	662	1.24	2.79	0.051
		3	811	0.85	4.02	0.035
		4	887	0.76	5.15	0.031

Continued

*Nozzle pressure was 75 psi.

TABLE 4.1 (Cont'd)

Cleaning Performance Test Results For 5/8 in. Fire Nozzle*

Nominal Mass Loading (g/ft^2)	Average Initial Mass $\bar{M}_o$ (g/ft^2)	Pass No.	Cleaning Rate R (ft^2/min)	Average Residual Mass $\bar{M}$ (g/ft^2)	Cumulative Effort E $\frac{(Noz\ Min)}{(10^3\ ft^2)}$	Average Residual Fraction $\bar{F}$
			PSR: (B) 88-177 μ			
50.0	50.5	1	403	2.22	2.48	0.044
		2	532	2.02	4.36	0.040
50.0	50.5	1	719	8.84	1.39	0.18
		2	719	2.88	2.78	0.057
		3	787	1.97	4.05	0.039
		4	858	1.62	5.22	0.032
100.0	102.5	1	346	0.71	2.89	0.0069
		2	430	0.16	5.21	0.0015
100.0	102.06	1	619	25.21	1.62	0.25
		2	665	4.18	3.12	0.041
		3	1108	2.24	4.02	0.022
		4	831	1.63	5.22	0.016
			PSR: (C) 177-350 μ			
4.0	5.46	1	511	0.25	1.95	0.046
		2	665	0.13	3.46	0.024
4.0	5.29	1	1008	0.84	0.99	0.16
		2	1055	0.49	1.94	0.092
		3	1108	0.16	2.84	0.030
		4	1099	0.11	3.75	0.020
12.0	13.3	1	511	0.50	1.95	0.038
		2	604	0.15	3.61	0.011
12.0	11.78	1	917	1.93	1.09	0.16
		2	985	0.79	2.10	0.067
		3	1156	0.38	2.97	0.032
		4	1108	0.26	3.87	0.022

Continued

*Nozzle pressure was 75 psi.

TABLE 4.1 (Cont'd)

Cleaning Performance Test Results For 5/8 in. Fire Nozzle*

Nominal Mass Loading (g/ft^2)	Average Initial Mass, $\bar{M}_o$ (g/ft^2)	Pass No.	Cleaning Rate, R (ft^2/min)	Average Residual Mass, $\bar{M}$ (g/ft^2)	Cumulative Effort, E (Noz Min)/(10^3 ft^2)	Average Residual Fraction, $\bar{F}$
			PSR: (C) 177-350 μ			
24.0	23.53	1	380	0.30	2.63	0.013
		2	554	0.12	4.43	0.0051
24.0	24.2	1	782	3.36	1.28	0.140
		2	792	0.51	2.54	0.021
		3	869	0.27	3.69	0.011
		4	842	0.17	4.88	0.0070
50.0	48.1	1	369	0.27	2.71	0.0057
		2	532	0.14	4.59	0.0029
50.0	49.32	1	682	16.52	1.47	0.23
		2	782	0.79	2.74	0.016
		3	831	0.30	3.95	0.0061
		4	858	0.25	5.11	0.0051
			PSR: (D) 350-700 μ			
4.0	4.09	1	462	0.04	2.16	0.0089
		2	665	0.02	3.67	0.0057
4.0	4.28	1	937	0.66	1.07	0.16
		2	964	0.15	2.11	0.035
		3	985	0.07	3.12	0.017
24.0	23.4	1	451	0.26	2.22	0.011
		2	596	0.08	3.89	0.0035
24.0	23.36	1	831	2.97	1.20	0.13
		2	917	0.42	2.29	0.018

*Nozzle pressure was 75 psi.

TABLE 4.2

Comparison of Cleaning Performance Test Results for Fire Nozzle Vs Flare Nozzle*

Particle Size Range, PSR (code & μ)	Nominal Mass Loading M (g/ft^2)	Nozzle Type	Average Initial Mass, $\bar{M}_o$ (g/ft^2)	Pass No.	Cleaning Rate, R (ft^2/min)	Average Residual Mass $\bar{M}$ (g/ft^2)	Cumulative Effort, E $\frac{(Ncz\ Min)}{(10^3\ ft^2)}$	Average Residual Fraction $\bar{F}$
A								
44-88	24.0	Fire	24.0	1	459	1.78	2.23	0.074
				2	475	1.49	4.38	0.062
	24.0	Flare	24.1	1	404	0.41	1.77	0.017
				2	487	0.10	3.23	0.0041
B								
88-177	24.0	Fire	24.2	1	418	0.63	2.39	0.026
				2	496	0.41	4.41	0.017
	24.0	Flare	24.1	1	403	1.37	2.48	0.057
				2	405	0.75	4.68	0.031
C								
177-350	24.0	Fire	23.5	1	380	0.66	2.63	0.028
				2	554	0.26	4.44	0.011
	24.0	Flare	23.6	1	328	0.35	3.04	0.015
				2	554	0.31	4.85	0.013
	24.0	Flare**	24.1	1	422	0.072	2.37	0.003
				2	633	0.036	3.95	0.0015
D								
350-700	24.0	Fire	23.4	1	451	0.30	2.22	0.013
				2	596	0.11	3.89	0.0047
	24.0	Flare	23.4	1	323	0.35	3.10	0.0148
				2	515	0.19	5.04	0.0081

* Data derived from radiac readings.

** Pressure increased to 160 psi.

Note: Nozzle pressures were kept at 75 psi (100 gpm) for the fire nozzle and at 120 psi (55 gpm) for the flare nozzle.

where $\bar{M}$ is the average residual mass after reclamation (g/ft^2)

$\bar{M}_o$ is the average initial mass before reclamation (g/ft^2)

$\bar{I}$ is the corrected* average residual count rate after reclamation (cpm)

$\bar{I}_o$ is the corrected* average initial count rate before reclamation (cpm)

F is the fraction of fallout simulant remaining on the asphalt pavement after reclamation. The average residual fraction, $\bar{F}$, is computed by either of the formulae:

$$\bar{F} = \bar{I}/\bar{I}_o \text{ or } \bar{F} = \bar{M}/\bar{M}_o \qquad (4.2)$$

Cumulative effort (E) is a measure of work expended per unit area. Each entry includes the effort expended for the pass shown, plus that for all previous passes. For convenience, E is given in terms of (nozzle-minutes)/10^3 ft^2.

4.2 INTERACTION OF ENVIRONMENTAL AND OPERATIONAL PARAMETERS

The results from Tables 4.1 and 4.2 have been used to construct a series of performance curves showing average residual mass $\bar{M}$ as a function of firehosing effort E. Cleaning theory predicts that with the increased expenditure of effort (by repeated firehosing passes), $\bar{M}$ will approach a minimum value. Therefore the shape, and particularly the slope, of these curves demonstrate how effectively firehosing achieves this minimum.

The curves have been organized into four sets to reveal the effects of hosing rate, PSR, mass loading, and stream pattern on firehosing performance. All four effects are discussed and evaluated in the following sections.

*Corrected for instrument calibration, background radiation, and isotope decay effects.

4.2.1 Effects of Hosing Rate

Twelve pairs of curves are grouped into Figs. 4.1 - 4.8 according to PSR. Each pair of curves shows the effect of firehosing rate on selected nominal mass loadings, at the slow (visually-controlled) rate of 350-650 ft^2/min and at the fast rate of 600-1150 ft^2/min.

The generally superior performance of the slow hosing rate indicates the rate dependence of cleaning effectiveness. In only three cases (Figs. 4.1, 4.2 and 4.5) the fast rate appeared to be equal to or slightly better than the slow rate. However, all the remaining curves demonstrate that, for equal effort, several passes at a fast rate are not as profitable as fewer passes at a slower rate. In addition it is too demanding for firehosing teams to maintain the fast rate throughout a work period of several hours. For these reasons the remainder of the analysis appearing in this chapter will be confined to tests conducted at the slow (visual) rate.

4.2.2 Effects of Particle Size Range

Figs. 4.9, 4.10 and 4.11 show the effects of PSR on performance for nominal mass loadings 4, 24, and 50 g/ft^2, respectively. The consistent ranking of the curves, for all three mass loadings, demonstrates that the removal effectiveness is a direct function of particle size, that is, the residual mass (and the residual fraction) decreased as the PSR increased.

Although the ranking of the curves by PSR is consistent, the variation in the spread between adjacent curves is not. Comparison of Figs. 4.9 and 4.10 shows that as particle size increases the spread increases for a nominal mass loading of 4 g/ft^2 and decreases for a nominal mass loading of 24 g/ft^2. This reversal in trend suggests that the degree to which particle size affects performance may depend upon mass loading. The evidence, however, is not conclusive.

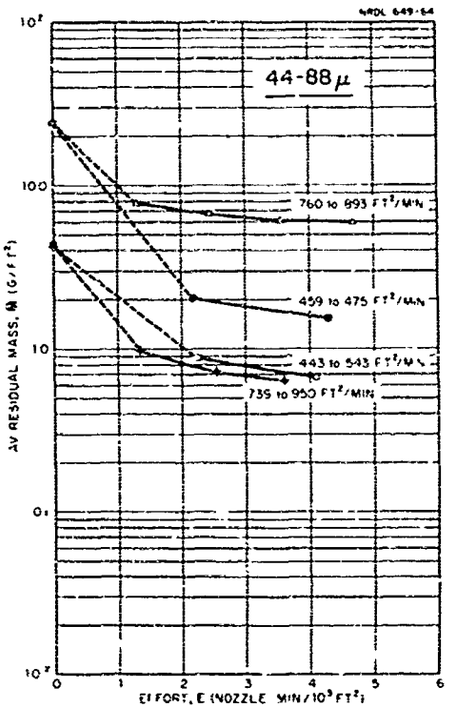

Fig. 4.1 Effect of Hosing Rate on Performance, Nominal Mass Loading 4 & 24 g/ft^2.

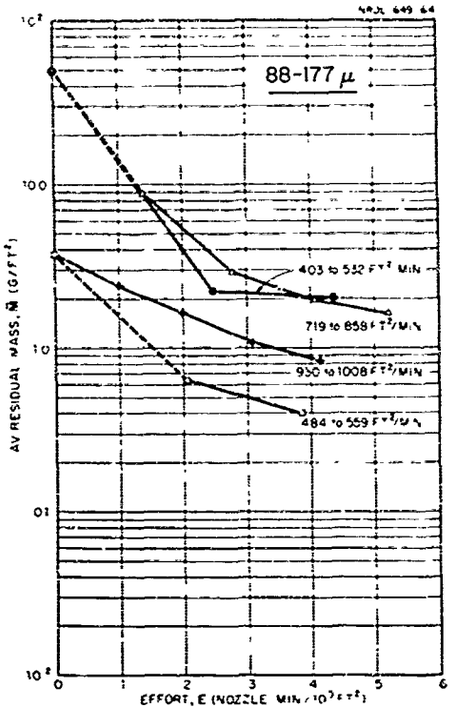

Fig. 4.2 Effect of Hosing Rate on Performance, Nominal Mass Loading. 4 & 50 g/ft^2.

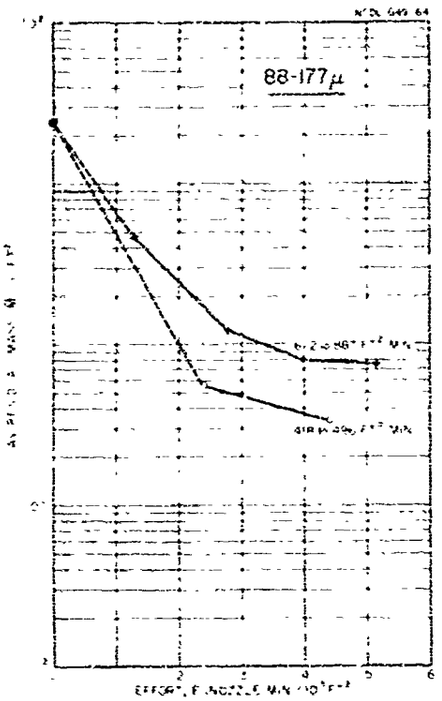

Fig. 4.3 Effect of Hosing Rate on Performance, Nominal Mass Loading 24 g/ft^2.

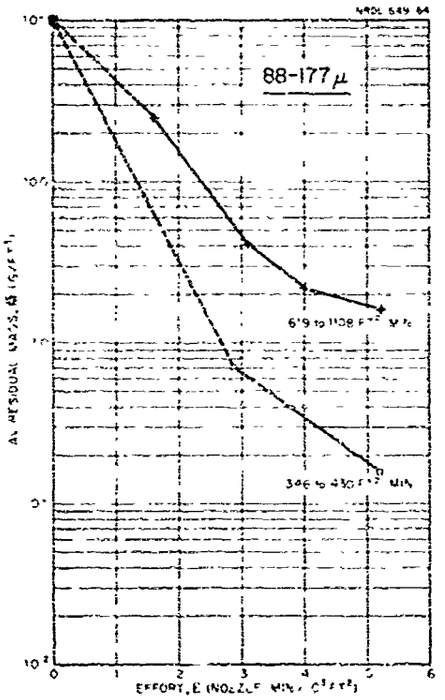

Fig. 4.4 Effect of Hosing Rate on Performance, Nominal Mass Loading 100 g/ft^2.

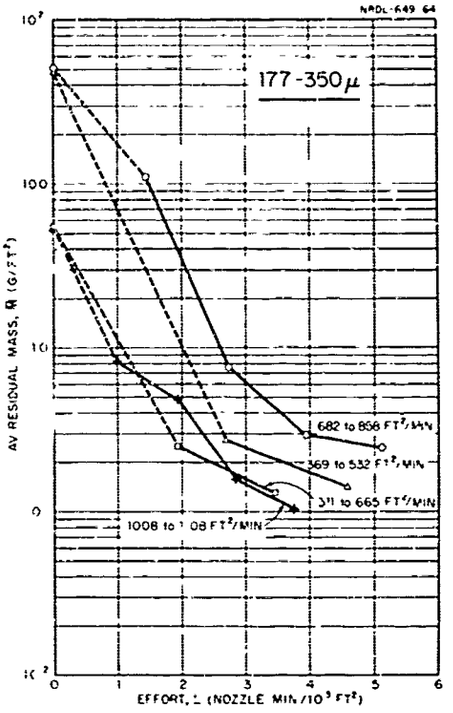

Fig. 4.5 Effect of Hosing Rate on Performance, Nominal Mass Loading 4 & 50 g/ft^2.

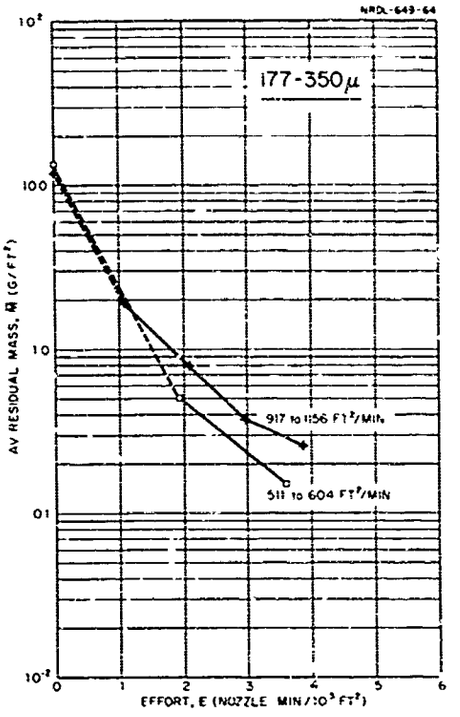

Fig. 4.6 Effect of Hosing Rate on Performance, Nominal Mass Loading 12 g/ft^2.

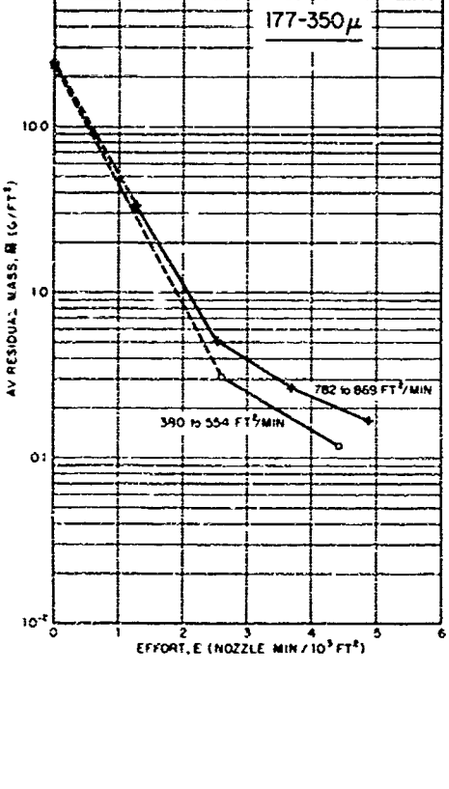

Fig. 4.7 Effect of Hosing Rate on Performance, Nominal Mass Loading 24 g/ft^2.

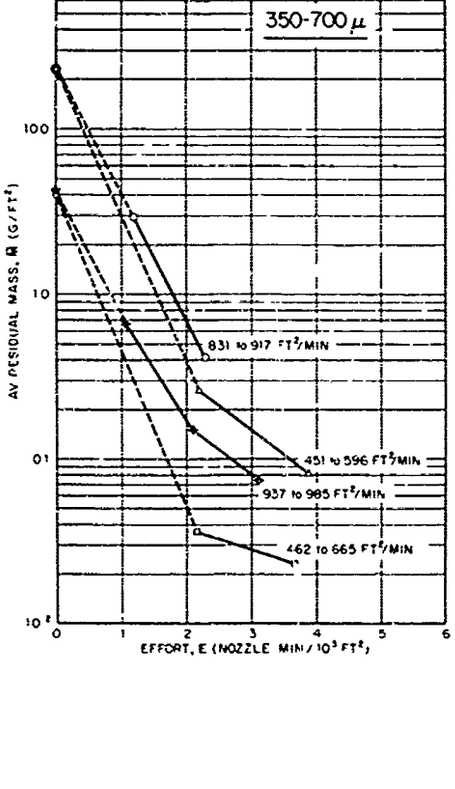

Fig. 4.8 Effect of Hosing Rate on Performance, Nominal Mass Loeding 4 & 24 g/ft^2.

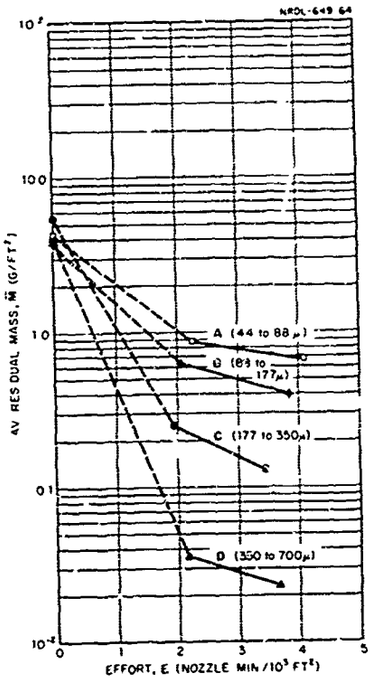

Fig. 4.9 Effect of Particle Size Range on Performance, Nominal Mass Loading 4 g/ft^2.

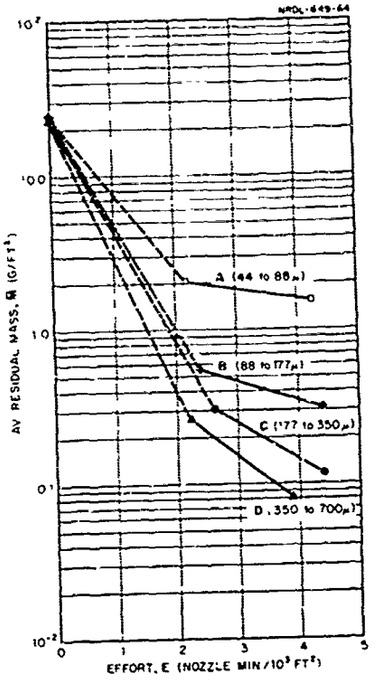

Fig. 4.10 Effect of Particle Size Range on Performance, Nominal Mass Loading 24 g/ft^2.

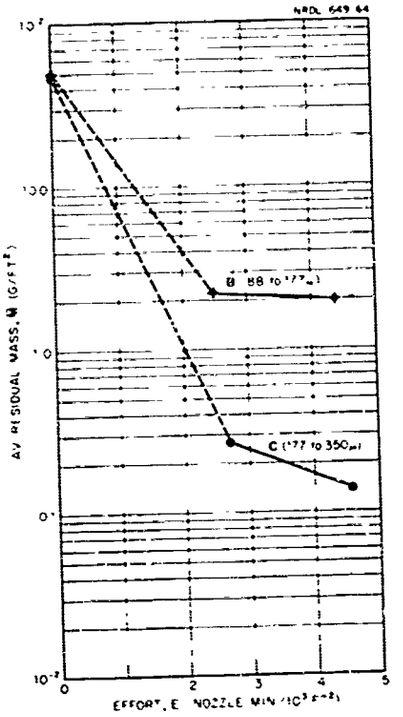

Fig. 4.11 Effect of Particle Size Range on Performance, Nominal Mass Loading 50 g/ft^2.

In general, the performance curves diverge with increased effort and the slopes increase with increased PSR. This means that additional effort is more profitable when the larger particle sizes are being fire-hosed. For example, comparing Curves A and C in Fig. 4.10, when the effort increased from 3 to 4, the residual mass decreased 11 % for Curve A and 44 % for Curve C.

4.2.3 Effects of Mass Loading

The performance curves in Figs. 4.12 to 4.15 are grouped according to PSR to disclose any effects due to mass loading. Plots of residual mass versus effort exhibited no consistent trends that could be attributed to initial mass loading. Fig. 4.12 is a typical example.

In order to demonstrate better the effects of mass loading, performance data were replotted in Figs. 4.13 - 4.15 as curves of average residual fraction $\overline{F}$ versus effort E. This in effect normalized all the performance curves to a common $\overline{F}$ value of $\overline{M}/\overline{M}_o$ equal to 1.0 when E equals zero. In general, it is evident from these plots that the average residual fraction $\overline{F}$ decreases (effectiveness improves) with increasing mass loading. An exception for PSR B is reflected in Fig. 4.14 where the 50-g/ft^2 curve is out of position. From the foregoing it may be said: As the initial mass loading, M_o, increases, the relative removal effectiveness (as measured by the ratio of M/M_o) improves, whereas the absolute effectiveness (as measured by residual mass M) may not.

4.2.4 Effects of Stream Pattern

Because it was found that project personnel were not required to assist in the preparation of simulant before noon on production Mondays, and because sufficient simulant was always left over from the scheduled tests of the previous week, a special series of tests was conducted with the flare nozzle. This made it possible to observe the effects of the flare nozzle's flat fan-shaped pattern and compare them with those of the fire nozzle's slender cone-shaped pattern. A nominal

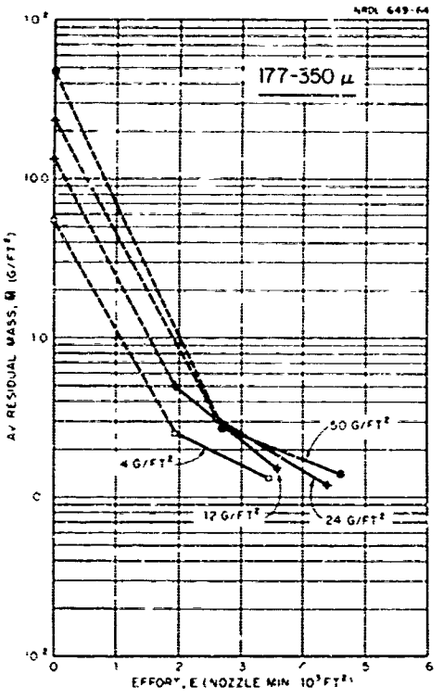

Fig. 4.12 Effect of Mass Loading on Performance.

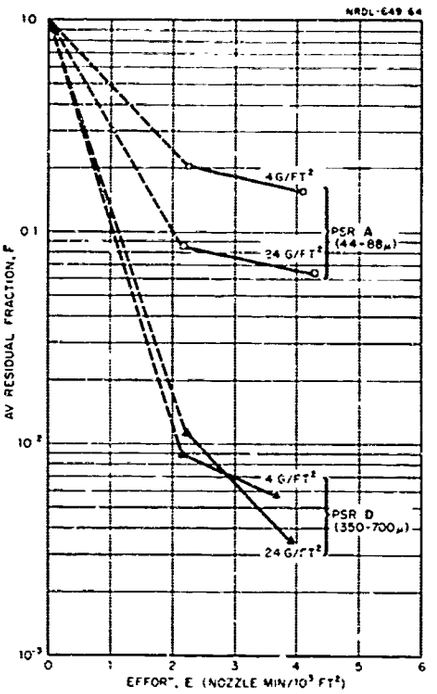

Fig. 4.13 Effect of Mass Loading on Performance.

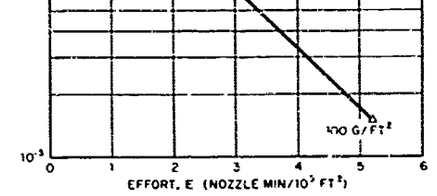

Fig. 4.14 Effect of Mass Loading on Performance.

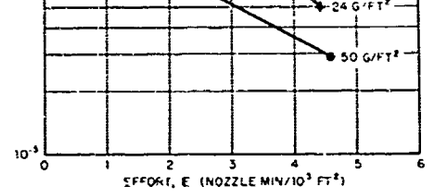

Fig. 4.15 Effect of Mass Loading on Performance.

mass loading of 24 g/ft^2 was spread for each of the fire flare nozzle tests.

Since a given set of test runs had to be completed by noon of each production Monday, it was impossible to spend the two or three hours required to make directional surveys with the shielded gamma detector. Therefore, the radiation surveys were made with the AN/PDR 27-C radiac. To be consistent, data from the fire nozzle tests referenced in this section were also based on radiac data.

The performance curves in Fig. 4.16 - 4.19 compare the stream pattern effects of the 5/8-in. fire nozzle to those of the flare nozzle. At nozzle pressures of 75 psi and 120 psi, for fire and flare nozzle, respectively, the latter was definitely superior during the removal of PSR A. The two nozzles were practically equal for PSR C. PSR's B and D were more effectively removed by the fire nozzle. However, when the nozzle pressure of the flare nozzle was increased from 120 to 160 psi (which provided a thrust equal to that of the 5/8-in. fire nozzle at 75 psi), its effectiveness improved by a factor of 6 to 7 (see Fig. 4.18). This increased effectiveness of the flare nozzle with PSR C could extend to the other PSR's. If it does, the flare nozzle may prove superior to the fire nozzle at the same thrust value. This can be determined by further testing of the flare nozzle at the higher pressure of 160 psi.

4.3 ASSESSMENT OF ERROR

No tests were run when the wind velocity was over 3 knots. Therefore the error due to particle size fractionation of the fallout simulant during and after spreading operations was negligible. This precaution also reduced errors in obtaining initial mass loading, $\bar{M}_o$. Values for the latter were determined by direct weighing methods.

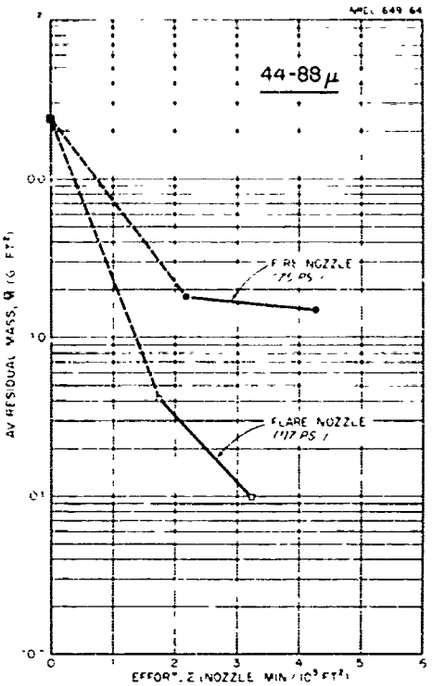

Fig. 4.16 Effects of Stream Pattern on Performance.

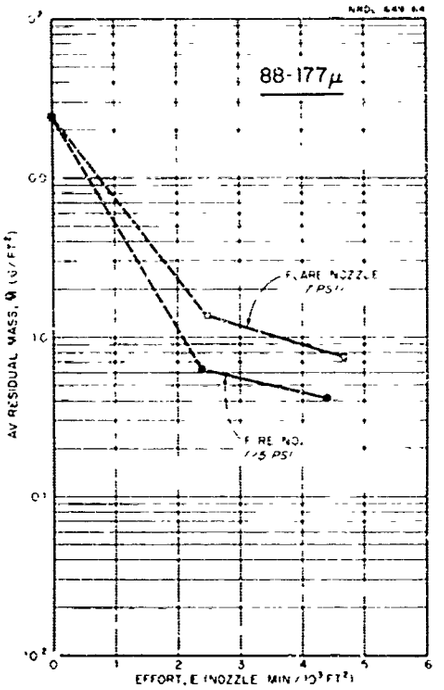

Fig. 4.17 Effects of Stream Pattern on Performance.

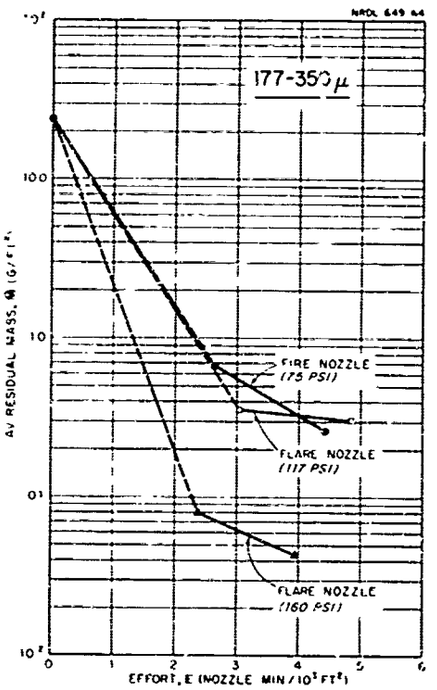

Fig. 4.18 Effects of Stream Pattern on Performance.

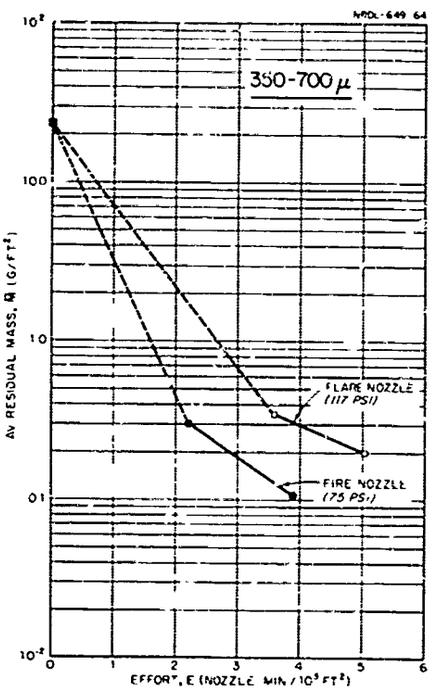

Fig. 4.19 Effects of Stream Pattern on Performance.

Because the scales could be read to the nearest half pound, the error in $\bar{M}_o$ was usually less than $\pm$ 5 %.

In the case of the residual mass determinations, the error was considerably larger. This was caused by a combination of direct and indirect sources of error. As described in Section 4.1, residual mass is not measured as such but must be estimated on the basis of radiation readings used in conjunction with Eq. 4.1.

$$\bar{M} = \bar{M}_o \quad (\bar{I}/\bar{I}_o)$$

On the average, initial and residual levels $\bar{I}_o$ and $\bar{I}$ each reflect the $\pm$ 15 % error inherent in the shielded gamma detector used in their measurement. These errors combine with that noted for $\bar{M}_o$, such that the rms error in $\bar{M}$ is approximately $\pm$ 22 %.

Still further error was introduced into residual mass derivations by virtue of the following. As shown in Appendix C, the specific activity increased for smaller particles within a given PSR. However, firehosing demonstrated greater removal effectiveness against the larger and less radioactive particles. This meant that a disproportionate quantity of small but more radioactive particles usually were left after hosing. This resulted in $\bar{I}$ values that were too high. Hence, estimates of $\bar{M}$ (from Eq. 4.1) also were high.

The magnitude of this particular effect is indeterminate for two reasons. First, although the 4-pi ionization chamber used to obtain specific activity was accurate to within $\pm$ 2 %, relative values varied by factors of 1.5 to 5, depending upon the PSR being analysed (see Figs. C.1 and C.2, Appendix C). Second, the effect of increased PSR on firehosing effectiveness is known only in a qualitative way. It can be said only that the net effect results in conservative estimates of residual mass, $\bar{M}$, and, therefore, of firehosing effectiveness.

Transfer of activity from the simulant to the test surface by leaching or ion exchange contributed less than 0.1 % error to the radiation measurements and, therefore, was considered negligible. These determinations were made routinely by project personnel as part of the required simulant analysis.

4.4 HOSING THEORY

It was noted earlier in Section 1.1 that, prior to these tests, a general theoretical explanation of fallout removal had been formulated. Moreover, an empirical equation had been developed which provided a reasonable fit to previous firehosing test data.[2] This expression was of the form

$$M = M^* + (M_o - M^*)\, e^{-3k\, E^{1/3}} \qquad (4.3)$$

where M is the residual mass (g/ft^2) after effort expenditure E

M^* is the residual mass (g/ft^2) after an infinite effort expenditure

M_o is the initial mass level (g/ft^2)

k is the proportionality constant expressing removal rate

E is the effort expended (nozzle min/10^3 ft^2)

$e^{-3k\, E^{1/3}}$ is the fraction of removable mass remaining after the expenditure of effort E.

The data from the current tests furnished values for M, M_o and E. The experiment was not designed to measure directly either M^* or k. Since there are two unknowns, Eq. 4.3 must be solved by successive approximations. This was readily accomplished on the NRDL IBM-704 computer.

A solution was attempted for each test. In some cases, as many as 100 iterations were required in order for the equation to close and give consistent values for M* and k. Each closure meant that Eq. 4.3 could be made to fit the data, for that particular test, on an M vs E plot of reclamation performance.

Table 4.3 contains the results of the computer equation-fitting process. Comparing the various ratios of closures to attempts, it is seen that the equation fitted data from 9 of 16 slow-rate tests, while only 2 out of 12 attempts were successful for tests conducted at the fast rate. From this it appears that Eq. 4.3 is more suited to describing the performance of hosing at the slow (visual) rate. However, it should be remembered that slow-rate tests required only 2 hosing passes whereas fast-rate tests required at least 3 and usually 4 passes. Since equation-fitting becomes more difficult as the number of data points increase, it is very possible that the sharp drop in the ratio of closures to attempts was the result of extra passes rather than a faster rate.

The resultant values of k and M* are shown in the last two columns of Table 4.3. It is evident that k tends to increase as PSR increases. Since k is by definition a measure of method efficiency[2], this trend is consistent with the finding noted earlier in Section 4.2.2. That is, coarse particles were more readily removed than fine particles. There are some weak indications that M* decreases with increasing PSR, and that both k and M* increase with initial mass loading for a given PSR. However, the data are so limited that only the possibility of such trends can be suggested.

If only the slow-rate tests are considered, the effects of nozzle design become apparent. The equation provided a fit to 50 % (6 of 12) of fire nozzle tests. The results are not conclusive, especially when it is realized that flare nozzle results depended upon radial rather than shielded measurements. Nevertheless the frequency of fit for the flare nozzle compares favorably with that obtained from street flusher results where similar nozzles were used.

TABLE 4.3

Computer Estimates of Cleaning Equation Coefficients

Test No.	Test Conditions PSR (μ)	Initial Mass (g/ft^2)	Equation Coefficients β: $\left(\frac{10^3}{Noz}\frac{ft^2}{Min}\right)^{1/3}$	M*: (g/ft^2)
5/8-In. Firenozzle, Slow Hosing Rate, Shielded γ Detector, 6 of 12 Attempts Closed				
A-1	44-88	4.26	1.3826	0.2177
A-3	44-88	24.04	2.4937	1.1401
B-2	88-177	24.2	3.1511	0.2020
B-3	88-177	50.5	3.7297	1.9103
C-4	177-350	48.1	3.9044	0.0659
D-1	350-700	4.09	4.0966	0.0157
5/8-In. Firenozzle, Fast Hosing Rate, Shielded γ Detector, 2 of 12 Attempts Closed				
A-2	44-88	4.43	1.6445	0.3013
A-4	44-88	24.1	1.7443	4.9035
Flare Nozzle, Slow Hosing Rate, Radiac, 3 of 4 Attempts Closed				
B-5	88-177	24.1	2.2269	0.1692
C-5	177-350	23.6	3.9495	0.2769
D-5	350-700	23.4	3.0277	0.0643

CHAPTER V

CONCLUSIONS AND RECOMMENDATIONS

5.1 CONCLUSIONS

1. In studying the effect of hosing rate on specific mass loadings in all particle size ranges it is apparent that:

a. In most cases the slow (visually controlled) rate will remove more material than the fast rate for the same amount of effort.

b. Hosing teams can operate at the slow rate for longer periods of time before tiring.

2. In general, removal effectiveness of firehosing improves with increased particle size range and increased mass loading. For the expenditure of an effort of 4 nozzle-minutes (12 man-minutes) per 10^3 ft^2, results ranged as follows:

Particle Size Range (μ)	Nominal Mass Loading (g/ft^2)	Removal Effectiveness (Residual Fraction)
44-88	4.0	0.16
	24.0	0.07
350-700	4.0	0.005
	24.0	0.003

3. The effects of stream pattern were inconclusive. It is quite possible that hosing performance can be improved through use of the flare nozzle, if the nozzle pressure is kept at 150 psi or greater.

4. The previously developed empirical cleaning formula (Eq. 4.3) appears to more nearly describe the performance of the flare nozzle than that of the fire nozzle.

5. The preliminary firehosing tests on streets determined that:

a. The most effective firehosing technique tested was frontal sweeping. In this technique the fire stream pushed the material down slope toward a collecting point (catch basin) located at the curb.

b. For a given fire nozzle and pressure, optimum stream range is dependent upon particle size.

c. For the 5/8-in. orffice fire nozzle operating at 75 psi, the optimum stream range for all practical purposes is greater than 15 ft and not more than 30 ft.

5.2 RECOMMENDATIONS

It is recommended that these firehosing studies be extended to include the following:

1. Conduct full-scale tests based on these engineering test results which will produce dose rate histories and allow the derivation of RN_2 factors for predicting exposure to recovery teams.

2. Investigate the promising performance of the flare nozzle on paved areas.

3. Compare the performance of the 5/8-in. fire nozzle and the flare nozzle on common roofing materials.

The above studies should include observance of the effects of PSR and mass loading.

REFERENCES

1. J. D. Sartor, et al., "Cost and Effectiveness of Decontamination Procedures for Land Targets", U.S. Naval Radiological Defense Laboratory, USNRDL-TR-196, 27 December 1957.

2. W. L. Owen, et al., "Performance Characteristics of Wet Decontamination Procedures - Stoneman II", U.S. Naval Radiological Defense Laboratory, USNRDL-TR-335, 21 July 1960.

3. C. F. Miller, "Fallout and Radiological Countermeasures - Volume I", Stanford Research Institute, SRI Project No. IM-4021, January 1963.

4. D. E. Clark Jr., W. C. Cobbin, "Removal Effectiveness of Simulated Dry Fallout from Paved Areas by Conventional Motorized Street Flusher", U.S. Naval Radiological Defense Laboratory, USNRDL-TR-797, 18 June 1964.

5. W. L. Owen, J. D. Sartor, "Radiological Recovery of Land Target Components, Complex III", U.S. Naval Radiological Defense Laboratory, USNRDL-TR-700, 20 November 1963.

6. W. L. Owen, J. D. Sartor, "Radiological Recovery of Land Target Components, Complex I and Complex II", U.S. Naval Radiological Defense Laboratory, USNRDL-TR-570, 25 May 1962.

7. D. E. Clark Jr., W. C. Cobbin, "Some Relationships Among Particle Size, Mass Level and Radiation Intensity of Fallout from a Land Surface Nuclear Detonation", U. S. Naval Radiological Defense Laboratory, USNRDL-TR-639, 21 March 1963.

APPENDIX A

PRELIMINARY TESTS

The experimental plan called for preliminary tests that would reveal the relationship between certain operational and environmental factors important to both the effectiveness and efficiency of firehosing operations. As indicated in Chapter II, the tests were carried out in two related phases. The first phase studied the behavior of water stream range (the distance between nozzle and stream impact point) as a function of particle size and nozzle orifice diameter. Using the results from first phase, the second phase compared the advantages of three different procedural approaches to firehosing for the purpose of selecting an optimum technique.

Since the desired information was obtainable by direct measurements and visual observations, no radioactive tracer was employed. The details of the two phases are presented in the following sections.

A.1 EFFECT OF STREAM RANGE

Limited results from Stoneman II tests in 1958 showed that reclamation performance of firehosing improved with increased stream range, L. No attempt was made to determine the optimum or limiting range, nor was it possible to investigate the influence of mass loading and particle size.

In 1961 the basic approach for obtaining this information was worked out. The test procedure was as follows: A strip of fallout

simulant (sized sand) measuring 4 ft wide and about 8 ft long was laid out on a paved area having a uniform surface condition. From a fixed height of 40 in., a standard fire nozzle was held by hand and aimed so the projected water stream would strike the near end of the sand strip. Without changing the angle of attack and hence the stream range, the stream was played back and forth across the width of the strip in four, 1-sec sweeps. The depth (distance forward), X, to which the stream penetrated the strip, leaving a visually clean pattern, was then measured and recorded. Test runs were repeated for stream ranges of 10 through 40 ft at 5-ft intervals. Complete series of tests were run for different simulant mass loadings and PSR's. Nozzle pressure was held constant for a given size of nozzle.

Unfortunately the data obtained from these particular tests were erratic, so the trials were abandoned. The tests showed that it was not possible to replicate a given run with a hand-held nozzle, especially when the water stream was deflected by gusts of wind. It was also found that, even under ideal conditions (no wind), the stream's cleaning pattern was not distinct enough to visually determine penetration depth unless the mass loading was approximately 200 g/ft^2.

For the current tests a special device was built to permit more precise control of the nozzle. It is called a turret nozzle (Fig. A.1). It consisted of an ordinary straight tapered fire nozzle attached to a special zero-torque swivel fitting. Nozzle and swivel assembly were fixed to a trailer-mounted pantograph linkage so that the stream attack angle could be changed to provide a variety of stream ranges. At the same time the nozzle height remained constant at 40 in. but was free to swing from side to side. The turret nozzle was fed by a 1-1/2-in. fire hose. This in turn was connected to a 500-gpm fire pump at a nearby fire hydrant.

In order to lessen any adverse wind effects, Camp Parks was thoroughly searched for a secluded test site. A suitable asphalt-paved

NRDL-649-64

Fig. A.1 Trailer-Mounted Turret-Nozzle Assembly. Operator is checking the nozzle pressure.

NRDL-649-64

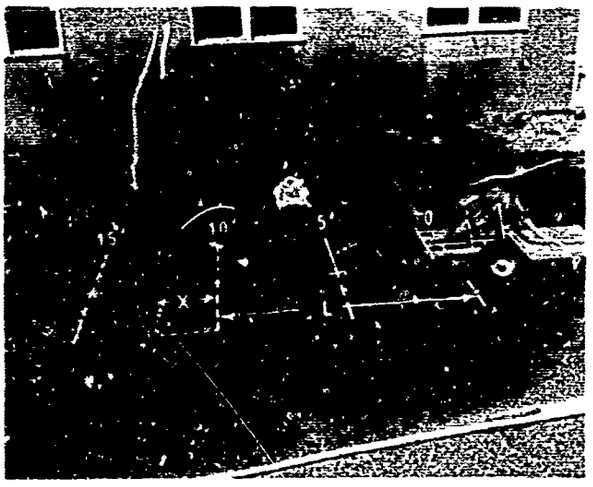

Fig. A.2 Typical arrangement of Simulant Strip and Turret-Nozzle showing relationship of penetration depth X and stream range L.

street was selected in a relatively protected enclosure formed by two 23-ft-high military barracks bordering the entire east and west sides. A wall 16 ft high by 60 ft wide was constructed between the south ends of the two barracks. Thus the test area was protected from winds prevailing in the morning but remained exposed to erratic gusts from all directions prevailing in the afternoon. An 8-x-120-ft test strip was located in the center of the 32-ft-wide crowned street. As shown in Fig. A.2, the test strip was divided into 5-ft increments for expediting stream range measurements. The asphalt surface was free of cracks, holes and patches, and was relatively flat and of uniform texture. Each side of the street beyond the strip sloped off into an unpaved but well drained gutter.

Using the above described turret nozzle and the 1961 test procedures (described in the beginning of this section), two complete series of test runs were conducted - each with a different size nozzle. The first series utilized a 1-1/2-in. fire nozzle with a 5/8-in. tip at a nozzle pressure of 75 psi*. The second series used a 1-1/2-in. fire nozzle with a 1/2-in. tip at a pressure of 117* psi. A nominal simulant mass loading of 200 g/ft^2 was used throughout for five different PSR's. The latter are indicated in the tables and graphs of test results.

Basic data from the stream range effects tests are given in Tables A.1 and A.2. Included are raw measurements of penetration depth (distance), X, as well as average values ($\bar{X}$) reduced from 2 and 3 runs per stream range. The average and the range of initial mass loading M_o and sand quality Q are also given for each particle size tested. Q is defined as the percentage of sand (by weight) falling within a prescribed nominal PSR.

*These pressures provided a relatively constant nozzle thrust of .45 to 50 lbs.

TABLE A.1

Basic Data From Stream Range Effects Tests, With a 5/8 in. Fire Nozzle

Particle Size Range: 44 - 88 μ

Initial Mass Loading, M_o (Average & Range): 204 (190 to 215) g/ft^2
Quality of Sand, Q (Average): 95 %

Stream Range, L (ft)								
10	15	20	25	30	35	40	45	50
Penetration Depth, X (ft)								
6.0	8.5	8.7	8.5	8.0	6.0	5.0	6.5	
6.0	8.5	8.8	8.0	7.0	6.5	6.0	6.0	
		9.0	8.5	8.0	6.0	6.3	5.8	
Average Penetration Depth, $\bar{X}$ (ft)								
6	8.5	8.8	8.3	7.7	6.2	5.8	6.1	

Particle Size Range: 88 - 177 μ

Initial Mass Loading, M_o (Average & Range): 198 (193 to 201) g/ft^2
Quality of Sand, Q (Average & Range): 90 (89 to 93) %

Stream Range, L (ft)								
10	15	20	25	30	35	40	45	50
Penetration Depth, X (ft)								
6.0	7.5	7.8	7.8	7.8	6.5	6.0		
6.0	7.7	8.5	8.5	8.0	7.0	6.3		
	7.7	8.5	8.3	7.7	6.8	6.2		
Average Penetration Depth, $\bar{X}$ (ft)								
6.0	7.6	8.3	8.2	7.8	6.8	6.2		

Continued

TABLE A.1 (CONT'D)

Particle Size Range: 177 - 350 μ

Initial Mass Loading, M_o (Average & Range): 198 (185 to 204) g/ft^2
Quality of Sand, Q (Range): 36 to 90 %*

Stream Range, L (ft)								
10	15	20	25	30	35	40	45	50
Penetration Depth, X (ft)								
3.8	4.8	5.8	6.8	5.0	4.0	4.7	4.5	2.7
3.8	5.2	6.1	5.8	4.8	5.0	4.8	4.5	3.5
			6.0		4.8			
Average Penetration Depth, $\bar{X}$ (ft)								
3.8	5.0	6.0	6.2	4.9	4.6	4.8	4.5	3.3

Particle Size Range: 350 - 700 μ

Initial Mass Loading, M_o (Average & Range): 192 (187 to 195) g/ft^2
Quality of Sand, Q (Average & Range): 89 (88 to 90) %

Stream Range, L (ft)								
10	15	20	25	30	35	40	45	50
Penetration Depth, X (ft)								
4.0	4.4	4.7	5.0	4.8	4.1	3.7		
4.3	4.3	4.8	5.5	4.7	4.0	3.7		
Average Penetration Depth, $\bar{X}$ (ft)								
4.2	4.4	4.8	5.2	4.8	4.0	3.7		

Particle Size Range: 700 - 1400 μ

Initial Mass Loading, M_o (Average & Range): 205 (198 to 211) g/ft^2
Quality of Sand, Q (Average): 96 %

Stream Range, L (ft)								
10	15	20	25	30	35	40	45	50
Penetration Depth, X (ft)								
4.1	5.8	6.8	7.5	7.0	5.0	5.0		
5.0	5.4	6.5	8.0	7.0	5.8	5.0		
5.0	6.0	6.9	7.7					
Average Penetration Depth, $\bar{X}$ (ft)								
4.7	5.7	6.8	7.7	7.0	5.4	5.0		

*Due to lack of necessary sieve sizes, closer quality determination was not possible.

TABLE A.2

Basic Data From Stream Range Effects Tests, With a 1/2 in. Fire Nozzle

Particle Size Range: 44 - 88 μ

Initial Mass Loading, M_o (Average & Range): 207 (193 to 233) g/ft^2
Quality of Sand, Q (Average & Range): 89 (83 to 91) %

Stream Range, L (ft)								
10	15	20	25	30	35	40	45	50
Penetration Depth, X (ft)								
2.5	3.5	4.0	4.5	5.0	5.7	6.7	5.8	4.0
2.5	3.5	4.5	4.7	5.3	5.5	6.7		
		4.0						
Average Penetration Depth, $\bar{X}$ (ft)								
2.5	3.5	4.2	4.6	5.2	5.6	6.7	5.8	4.0

Particle Size Range: 88 - 177 μ

Initial Mass Loading, M_o (Average & Range): 199 (195 to 201) g/ft^2
Quality of Sand, Q (Average): 93 %

Stream Range, L (ft)								
10	15	20	25	30	35	40	45	50
Penetration Depth, X (ft)								
3.3	5.0	6.0	6.0	6.5	6.5	6.2	5.5	5.5
3.3	5.2	6.5	6.0	6.7	6.0	6.2	5.5	5.5
	5.0				6.5			
Average Penetration Depth, $\bar{X}$ (ft)								
3.3	5.1	6.2	6.0	6.6	6.3	6.2	5.5	5.5

Continued

TABLE A.2 (CONT'D)

Particle Size Range: 177 - 350 μ

Initial Mass Loading, M_o (Average & Range): 197 (187 to 221) g/ft^2
Quality of Sand, Q (Range): 37 to 90 %*

Stream Range, L (ft)								
10	15	20	25	30	35	40	45	50
Penetration Depth, X (ft)								
2.7	3.7	4.5	4.7	5.0	6.0	5.0	5.0	6.0
2.7	3.7	4.6	5.0	4.7	6.5	6.0	5.8	5.0
			4.7	4.7	6.3	5.5	5.8	5.5
Average Penetration Depth, $\bar{X}$ (ft)								
2.7	3.7	4.6	4.8	4.8	6.3	5.5	5.5	5.5

Particle Size Range: 350 - 700 μ

Initial Mass Loading, M_o (Average & Range): 198 (191 to 204) g/ft^2
Quality of Sand, Q (Average & Range): 86 (85 to 88) %

Stream Range, L (ft)								
10	15	20	25	30	35	40	45	50
Penetration Depth, X (ft)								
3.0	3.7	5.0	5.0	5.0	4.0	6.3	4.7	5.0
3.0	3.6	5.2	5.0	5.0	4.7	5.7	4.5	5.7
					4.7	6.5	5.0	5.0
Average Penetration Depth, $\bar{X}$ (ft)								
3.0	3.6	5.1	5.0	5.0	4.5	6.2	4.7	5.2

Particle Size Range: 700 - 1400 μ

Initial Mass Loading, M_o (Average & Range): 199 (192 to 213) g/ft^2
Quality of Sand, Q (Average): 96 %

Stream Range, L (ft)								
10	15	20	25	30	35	40	45	50
Penetration Depth, X (ft)								
3.0	4.5	5.7	6.1	7.0	6.0	7.7	5.2	
3.0	4.2	5.7	6.1	6.5	6.5	7.0	6.8	
	4.3			6.5	6.5	8.0	7.8	
							9.0	
							8.0	
Average Penetration Depth, $\bar{X}$ (ft)								
3.0	4.3	5.7	6.1	6.7	6.3	7.6	7.4	

*Due to lack of necessary sieve sizes, closer quality determination was not possible.

Figures A.3 through A.6 contain plots of average values found for penetration depth, X, against stream range, L. A comparison of the results obtained with the 5/8-in. fire nozzle on all five PSR's is presented in Fig. A.3 as a family of curves. Each curve exhibits a region of maximum penetration depth and then drops off with increasing stream range. The dotted portions are an attempt to locate optimum ranges on the assumption that the curves should fair smoothly through these critical data points.

The optimum range values corresponding to the maximum penetration values from these curves are tabulated below according to PSR. There are no strong correlations among the three variables represented. Optimum stream range appears to increase with PSR, while maximum penetration depth fluctuates between 5 and 9 ft. From these results it can be stated only that the optimum stream range for the 5/8-in. fire nozzle is probably greater than 15 ft and less than 30 ft, regardless of particle size.

Particle Size Range (Code & μ)	Region of Optimum Range (ft)	Maximum Penetration (ft)
A, 44-88	16-21	8.8
B, 88-177	19-25	8.3
C, 177-350	21-26	6.3
D, 350-700	24-28	5.2
E, 700-1400	24-28	7.8

It is apparent from Figs. A.4, A.5 and A.6 that results from the 1/2-in. fire nozzle tests were not totally satisfactory. The curves demonstrate none of the consistent form evident in Fig. A.3. Only the smallest PSR, i.e. A, exhibits a strong maximum penetration depth. Intermediate PSR's B, C, and D show rather indefinite regions of maximum X values. The largest PSR, E, indicates no positive maximum X value at all for the stream ranges tested. Taking peak X values from the curves as the best estimate of maximum penetration, the

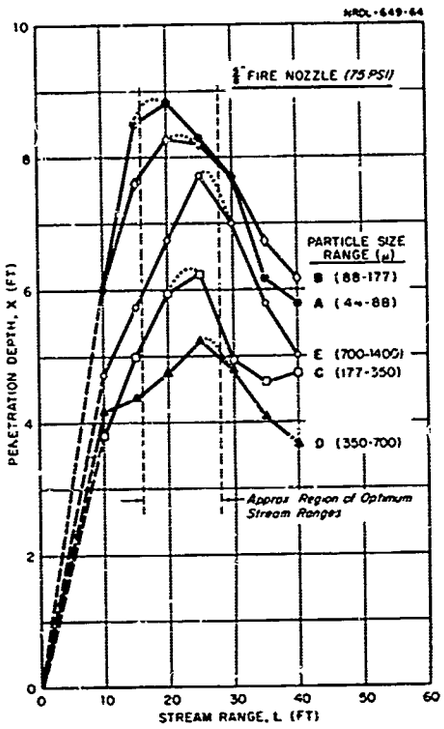

Fig. A.3 Optimum Stream Range as Determined From Depth of Penetration For Various Simulant Particle Sizes.

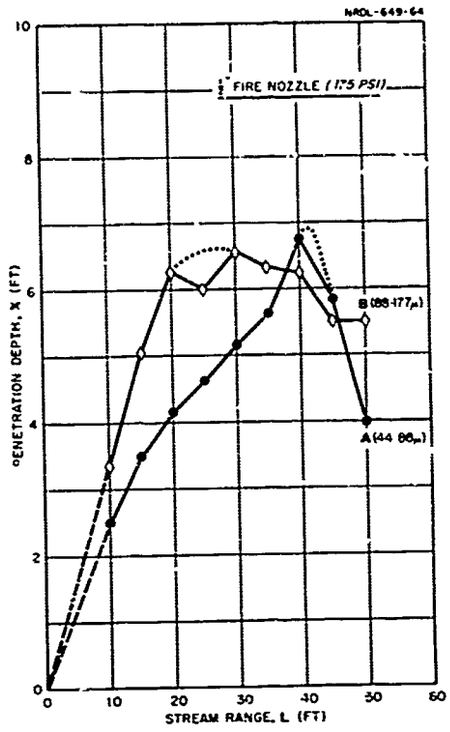

Fig. A.4 Stream Range Effects For Particle Size Ranges A and B.

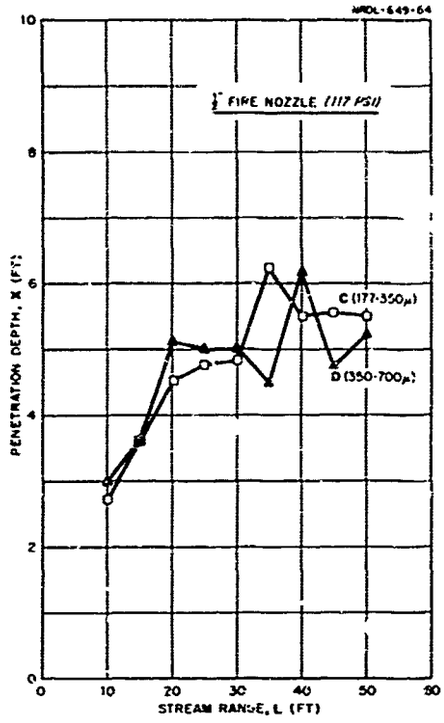

Fig. A.5 Stream Range Effects For Particle Size Range C & D.

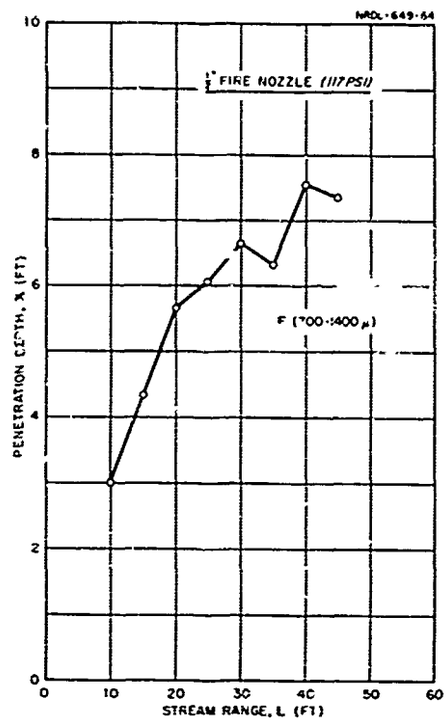

Fig. A.6 Stream Range Effects For Particle Size Range E.

optimum stream range appears to be between 30 and 40 ft. Whether the optimum stream range for the 1/2-in. nozzle is really greater than that for the 5/8-in. nozzle must remain in doubt. However, as concluded in the summary to this appendix, stream ranges beyond 30 ft are impractical. Hence, the continued search for the optimum stream range of the 1/2-in. fire nozzle becomes academic.

A.2 FIREHOSING TECHNIQUE

The fundamental approach to the removal of fallout by firehosing has remained essentially unchanged since the first shipboard experiments. These early tests demonstrated that both complete surface coverage and maximum effectiveness could be achieved by directing the waterstream like a gigantic broom. That is, the nozzle was played from side to side as the forward progress of the stream pushed all loosened contaminant before it. Prior to the present tests, the only significant improvement in this basic frontal-sweeping technique had been to increase the stream range. Results reported in Section A.1 provided the upper and lower limits for optimum stream ranges. Therefore, without introducing changes in firehosing equipment, the only other probable source of improvement lay in the firehosing technique itself.

Two techniques were developed and compared with frontal-sweeping to determine which one made the best use of the newly found optimum stream ranges. A schematic representation of all three techniques is given in Fig. A.7. Frontal-sweeping, of course, refers to the fundamental approach described in the beginning. This was the control or basis for comparison. The object of the parallel stripping technique was to reduce the mass buildup along the curb. Slant stripping was designed to take advantage of the cross-drainage caused by the street's crown. The three techniques were carried out in as realistic a manner as possible with the available man-power.

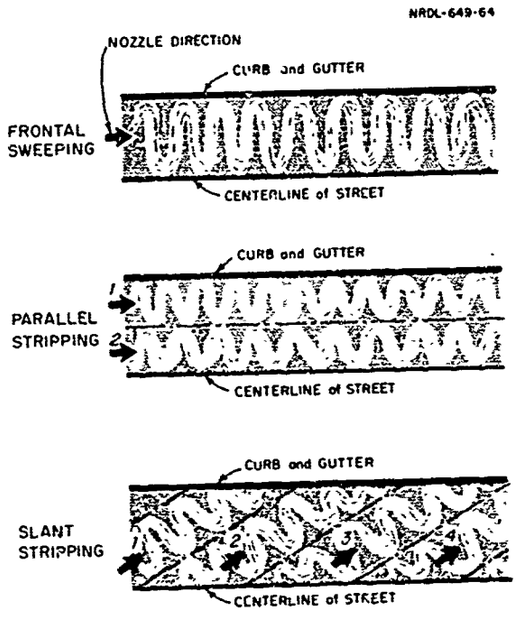

Fig. A.7 Comparison of Firehosing Techniques.

Tests were performed at the site used later for the principal firehosing experiment. Sand of one of the 5 PSR's was spread over an asphalt area 14 ft wide and 100 ft long. One nominal mass loading of 100 g/ft^2 was used throughout the series. The 5/8-in. orifice fire nozzle was used in eight tests. A ninth test was run to observe the performance of the flare nozzle.*

In all tests the nozzles were hand-held. A team of three men was required to control the nozzle and hose in carrying out the prescribed techniques. The fire nozzle was directed from an approximately constant height of 40-in. above the pavement. Fire nozzle pressure was maintained at 75 psi. Where possible an optimum stream range of 20 to 25 ft was maintained as a practical average value for all PSR's tested.

Test results are given in Table A.3 for five PSR's. It is apparent that the initial mass loadings (M_o) was consistently close to the nominal value of 100 g/ft^2. The quality (Q) of the sand was acceptable, though not high, for the smaller sizes. Total time (t) in minutes is shown together with the calculated rate (R) for each test run. Removal effectiveness was determined visually to be at least 95 % for all tests.

Only five test runs were necessary to demonstrate the general superiority of the basic technique, frontal sweeping. The results are grouped in Table A.3 above the dashed line. Consider first the three tests conducted with the fire nozzle on PSR E** sand. Comparison of either the times or rates shows that parallel stripping was considerably slower than the other two techniques. It was 21 % slower than frontal sweeping. After completion of the first strip adjacent to the curb, a full minute was required to drag the hose back to the starting point and commence removal of the second and last strip.

*See Section 3.2 for description of this special nozzle.
**It was discovered that this coarse sand was slowly grinding up the disperser impeller. Therefore, PSR E was not included in the principal tests, to save the equipment. This particle size is not of major interest in realistic reclamation situations.

TABLE A.3

Comparison of Hosing Techniques

Technique	PSR (code & μ)	M_o (g/ft^2)	Q (%)	t (min)	C (ft^2/min)
	Flare Nozzle: 150 Psi				
Frontal Sweeping	E, 700-1400	105	88	6.9	203
	5/8-in. Fire Nozzle: 75 Psi				
Frontal Sweeping	E, 700-1400	109.5	96	7.7	182
Parallel Stripping	E, 700-1400	100	96	9.8	143
Slant Stripping	E, 700-1400	92	96	5.8	241
Frontal Sweeping	C, 150- 300	105	89	6.1	229
Slant Stripping	C, 150- 300	109	86	6.7	209
Frontal Sweeping	A, 44- 88	105	78	3.6	389
Frontal Sweeping	B, 88- 177	104	87	4.2	333
Frontal Sweeping	D, 350-700	97	96	5.9	237

Even if this time loss were not included, parallel stripping would still have been the slowest technique.

Slant-stripping progressed 32 % faster than frontal-sweeping when used to remove sand of PSR E. However, comparison of these same techniques on PSR C indicated that slant stripping was 9 % slower. Apparently the PSR could be a determining factor as far as these two techniques were concerned. In order to be more conclusive the actual removal effectiveness would have to be determined. This was not possible.

Frontal-sweeping was chosen for the principal tests over slant-stripping because of other considerations. First, the latter method was observed to splatter fallout simulant on and beyond curbs, thus creating a contamination control problem. Second, it was not always possible to stand-off far enough to take advantage of the optimum stream range conditions. On open roads and highways, where there are no curbs and contamination beyond the shoulders is no problem, slant-stripping could undoubtedly be used to good advantage. In built-up areas where contamination control is important there appears to be no better technique than the time-proven frontal-sweeping.

In Table A.3 below the dashed line are the results of three tests constituting an attempt to observe the effects of optimum stream ranges on frontal-sweeping for the remaining three PSR's, A, B, and D. These results, together with those from frontal-sweeping of PSR's C and E, are indeterminate. The principal tests conducted later with radioactive tracer demonstrated that removal effectiveness improved as particle size increased, when hosing rate and mass loading were practically constant. For instance, effectiveness increased from 92 to 99 % as PSR increased from A to D, when firehosing a 24 g/ft^2 concentration at an average rate of 480 ($\pm$ 30) ft^2/min. In view of the large rate changes evidenced in the five preliminary test runs, no inferences are possible without measurements of actual removal effectiveness.

A final test run was made with the flare nozzle to see if it were a practical tool for reclaiming streets. Comparing the results in the upper half of Table A.3, this nozzle appears to be competitive with the fire nozzle, at least for sand in PSR E.

A.3 SUMMARY

Taken as a whole, the preliminary tests met the first two experimental objectives - if not always in a quantitative manner. The first phase established the upper and lower limits of optimum stream ranges for the 5 PSR's on the basis of penetration depth. The second phase confirmed the general superiority of the basic frontal-sweeping firehosing technique.

Although the penetration depth tests with the 1/2-in. orifice nozzle demonstrated high stream ranges, distances greater than about 30 ft are precluded for practical reasons. Nozzle operator visibility is not good enough beyond 30 ft to insure complete and effective removal by firehosing. In addition, it is difficult for the nozzle operator to judge stream ranges in excess of 30 ft.

APPENDIX B

SELECTION OF APPROPRIATE MASS LOADINGS

In a controlled experiment the investigator has some choice in the fallout simulant properties of particle size, mass loading and specific activity.* Sand simulant in five size ranges were available from Camp Parks simulant production facility. The first four sizes, extending from 44 μ to 700 μ are representative of material originating from the fallout cloud. These are the PSR's shown in Table 1.1 of the Introduction.

Unlike particle size, mass loading is limited only by the amount of sand available and the capability of the dispersing equipment. Therefore, it was necessary to work through a suitable fallout model in order to make realistic mass-loading selections for the four PSR's tested. Fortunately, Clark and Cobbin[7] had developed a simplified method for doing this using C. F. Miller's fallout scaling model**. From information conveniently provided in Ref. 7 it is possible to quickly correlate essential fallout properties with weapon yield and downwind distance.

By entering the fallout model with the desired PSRs from Table 1.1, the radiological conditions shown in the upper half of Table B.1 were derived. When restricted to these precise PSRs, the model provides a

---

* This property is discussed in Appendix C.

**The scaling factors associated with the fallout model when used in Ref. 7 do not necessarily reflect the model refinements reported in Ref. 3

TABLE B.1

Possible Radiological Conditions for Available Particle Size Ranges

Particle Size Range (Code & μ)	Weapon Yield (kt)	Downwind Distance (mi)	Standard Exposure Rate (r/hr)	Mass Loading (g/ft^2)
A, 44-88	10^5	258	6,000	7.5
B, 88-177	25,000	91	12,000	28
C, 177-350	750-1,000	26	2,400	14
D, 350-700	50-75	10	500	4.5
		At Peak Standard Exposure Rate		
B', 75-210	50,000-10^5	95-118	21,000-30,000	48-60
C', 165-360	250-1,000	19- 29	1,850- 2,700	9-14
D', 345-805	10-25	5.5-9.1	310-400	-4.5

comparatively small selection of mass loadings, i.e., 4.5 to 28 g/ft^2. In order to measure the effects of mass loading, it was necessary to test a broader range of values. At the same time, it was of interest to determine whether the model could be used further to establish criteria for selecting heavier mass loadings under conditions including PSRs approximating those to be tested.

From the information tabulated in Appendix C of Ref. 7 it was possible to determine the behavior of mass loading with downwind distance. The family of curves in Fig. B.1 shows this relationship for various explosive yields. It is apparent from this plot that, for yields greater than 25 KT, a secondary maximum mass loading occurs at the same location as the downwind-peak standard-exposure-rate. From the fallout model it was found that three of these peak conditions could be attained from fallout closely approximating the three larger PSR's. The latter have been arbitrarily coded as B', C', and D' and entered together with the required radiological conditions in the lower half of Table B.1. The maximum mass loadings shown in Table B.1 for these PSR's do not differ markedly from their counterparts in the upper part of the table - except for PSR's B and B'. In this case the mass loading is practically doubled. However, both PSR's C and D now include a peak condition. PSR A does not.

Combination of the respective available and approximate PSR's established the upper limits of the appropriate mass loading.* The lower limits were determined from Fig. B.1, where the peak mass loadings for the lower yields become practically constant at about 4.5 g/ft^2. Although this was an arbitrary limit it coincided with the minimum amount of simulant that could be uniformly spread with present equipment. To further simplify simulant dispersal problems, the mass loadings in Table B.1 were rounded off to the nearest 4, 12, 24, or 50 g/ft^2. This resulted in the following selections:

*For fallout deposits resulting from a single detonation.

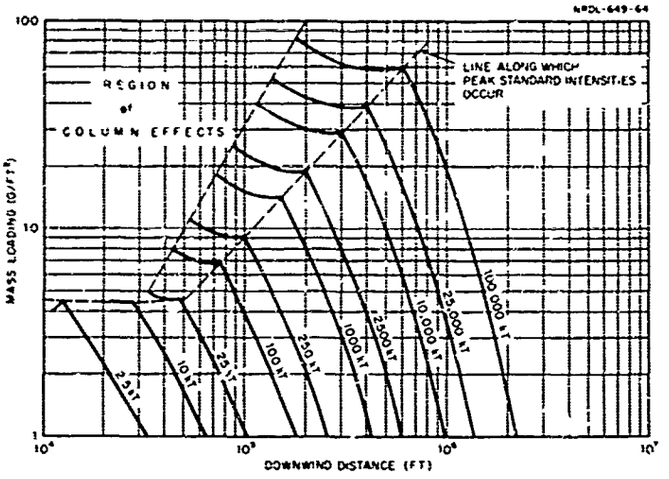

Fig. B.1 Mass Loadings Predicted at Various Distances From Specific Explosive Yields.

Particle Size Range (Code & μ)	Mass Loading (g/ft^2)				
	4	12	24	50	100
A, 44 - 88	(X)	-	X	-	-
B, 88 -177	X	-	(X)	X	X
C, 177 -350	X	(X)	X	X	-
D, 350 -700	(X)	-	X	-	-

Note: Parentheses enclose selections determined from available PSRs. Underlined selections correspond to peak conditions determined from approximate PSRs.

In order to have a control test condition at one mass loading it was decided to test the four PSRs at 24 g/ft^2. This, plus the two extra selections of 100 g/ft^2 for PSR B and 50 g/ft^2 for PSR C, allowed, in part, for the possible increase in expected mass loadings due to multiple bursts. Because it did not place any extra demand upon simulant production, a secondary control was established at the 4 g/ft^2 mass loading.

APPENDIX C

FALLOUT SIMULANT ANALYSIS

Six batches of fallout simulant were used in the principal experiment. Samples of each batch were analyzed to correlate pertinent physical and radiological properties with particle size distribution. The latter was established according to A.S.T.M. procedures. The mass of each particle size fraction was determined to the nearest 0.01 g. The activity of each size fraction and of the total sample was measured in a 4-pi ion chamber.

Tables C.1 through C.6 present the results of the analyses. The bottom of each table shows the control percentage of mass and activity, which includes the significantly contributing size fractions of each batch sample*. Standard correction factor and background apply to the 4-pi ion chamber. Both are referred to the same zero time as the specific activity of the simulant (1200 hours on day of simulant production).

Ideally, tagging the bulk carrier would give a constant specific activity (μc/g) for all particulate in a given particle size range. If the particles were covered uniformly with the La^{140}, the radioactivity on a particle would be proportional to the surface area. This activity can be related to the volume or mass (assuming uniform material density) for spherical particles of diameter, d, as follows:

$$\frac{\% \text{ Activity}}{\% \text{ Mass}} \propto \frac{\text{Surface}}{\text{Volume}} = \frac{\pi d^2}{\pi d^3/6} = 6/d$$

$$\text{or} \quad \% A/\% M = K(6/d) = K'/d \qquad (C.1)$$

*These are shown in the tables between the lines inserted into certain of the columns.

TABLE C.1

Simulant Analysis, Batch #1, PSR: C, 177-350 μ

Particle Size (μ)	Particle Mid Range (μ)	Weight (g)	Percent Mass	Percent Activity	% Activity / % Mass	Reciprocal of Particle Size $10^3/d$ (μ^{-1})
+ 500		0.02	0.02	0.04	2.00	
+ 420	460	0.11	0.11	0.11	1.00	2.17
+ 350	387	5.61	5.62	4.37	0.78	2.58
+ 297	326	22.47	22.51	19.04	0.85	3.06
+ 250	274	40.74	40.83	37.46	0.92	3.64
+ 177	214	28.55	28.60	33.72	1.18	4.67
+ 149	163	1.66	1.66	3.50	2.11	6.13
+ 125	137	0.27	0.27	0.75	2.78	7.29
Pan		0.38	0.38	1.00	2.63	
Control Percentage:			91.94	90.22		

Standard Correction Factor: 670/680 = 0.986
Background (ma): 25×10^{-11}
Specific Activity (μc/g): 68.4 at 1200 9/16/63

TABLE C.2

Simulant Analysis, Batch #2, PSR: D, 350-700 μ

Particle Size (μ)	Particle Mid Range (μ)	Weight (g)	Percent Mass	Percent Activity	% Activity / % Mass	Reciprocal of Particle Size $10^3/d$ (μ^{-1})
+ 707		0.06	0.06	0.04	0.67	
+ 595	651	0.33	0.33	0.27	0.82	1.54
+ 500	548	5.81	5.84	5.00	0.86	1.82
+ 420	460	25.66	25.78	22.98	0.89	2.17
+ 354	387	50.44	50.68	49.21	0.97	2.58
+ 297	326	10.61	10.66	13.74	1.29	3.07
+ 250	274	3.13	3.14	3.90	1.24	3.65
+ 210	230	1.19	1.20	1.37	1.14	4.35
Pan		2.30	2.31	3.50	1.52	
Control Percentage:			92.96	90.93		

Standard Correction Factor: 670/640 = 1.04687
Background (ma): 25×10^{-11}
Specific Activity (μc/g): 58.6 at 1200 9/23/63

TABLE C.3

Simulant Analysis, Batch #3, PSR: A, 44-88 μ

Particle Size (μ)	Particle Mid Range (μ)	Weight (g)	Percent Mass	Percent Activity	% Activity / % Mass	Reciprocal of Particle Size $10^3/d$ (μ^{-1})
+ 105		4.28	4.29	2.53	0.59	
+ 88	97	3.05	3.06	3.14	1.03	10.31
+ 74	81	25.40	25.45	21.13	0.83	12.35
+ 62	68	24.54	24.59	22.21	0.90	14.71
+ 53	58	18.28	18.32	18.70	1.02	17.24
+ 44	49	20.44	20.48	24.21	1.18	20.41
Pan		3.80	3.81	8.08	2.12	
Control Percentage:			99.84	86.25		

Standard Correction Factor: 670/670 = 1.0
Background (ma): 25×10^{-11}
Specific Activity (μc/g): 68.4 at 1200 10/7/63

TABLE C.4

Simulant Analysis, Batch #4, PSR: B, 88-177 μ

Particle Size (μ)	Particle Mid Range (μ)	Weight (g)	Percent Mass	Percent Activity	% Activity / % Mass	Reciprocal of Particle Size $10^3/d$ (μ^{-1})
+ [illegible]9		0.75	0.75	0.41	0.55	
+ 177	194	1.32	1.33	0.96	0.72	5.15
+ 149	163	Trace	-	-	-	6.13
+ 125	137	44.32	44.57	37.90	0.85	7.30
+ 105	115	30.18	30.35	31.22	1.03	8.70
+ 88	97	18.55	18.65	22.41	1.20	10.31
+ 62	75	4.10	4.12	6.60	1.60	13.33
Pan		0.22	0.22	0.50	2.27	
Control Percentage:			93.57	91.53		

Standard Correction Factor: 670/667 = 1.00449
Background (ma): 25×10^{-11}
Specific Activity (μc/g): 24.5 1200 10/14/63

TABLE C.5

Simulant Analysis, Batch #5, PSR: C, 177-350 μ

Particle Size (μ)	Particle Mid Range (μ)	Weight (g)	Percent Mass	Percent Activity	% Activity / % Mass	Reciprocal of Particle Size $10^3/d$ (μ^{-1})
+ 500		0.06	0.06	0.18	3.0	
+ 420	460	0.53	0.54	0.32	0.59	2.17
+ 350	385	10.86	10.97	7.32	0.67	2.60
+ 297	324	41.89	42.30	31.74	0.75	3.09
+ 250	274	21.84	22.05	23.76	1.08	3.65
+ 177	214	20.27	20.47	27.81	1.36	4.67
+ 149	163	1.63	1.65	3.88	2.35	6.13
+ 125	137	0.50	0.50	1.35	2.70	7.30
Pan		1.45	1.46	3.62	2.48	
Control Percentage:			95.79	90.63		

Standard Correction Factor: 670/668 = 1.00299
Background (ma): 25×10^{-11}
Specific Activity (μc/g): 58.6 at 1200 10/21/63

TABLE C.6

Simulant Analysis, Batch #6, PSR: B, 88-177 μ

Particle Size (μ)	Particle Mid Range (μ)	Weight (g)	Percent Mass	Percent Activity	% Activity / % Mass	Reciprocal of Particle Size $10^3/d$ (μ^{-1})
+ 210		3.03	3.04	2.74	0.90	
+ 177	194	5.05	5.06	4.11	0.81	5.15
+ 149	163	19.81	19.85	16.87	0.85	6.13
+ 125	137	25.83	25.89	23.75	0.92	7.30
+ 105	115	27.23	27.29	27.49	1.01	8.70
+ 88	97	14.40	14.43	17.50	1.21	10.31
+ 62	75	4.36	4.37	7.37	1.69	13.33
Pan		0.07	0.07	0.17	2.43	
Control Percentage:			87.46	85.61		

Standard Correction Factor: 670/670 = 1.0
Background (ma): 40×10^{-11}
Specific Activity (μc/g): 45.6 at 1200 11/11/63

where K' (6 K) is a proportionality constant between specific activity ($\mu c/g$) and the reciprocal of the particle diameter (1/d). The idealized relationship of Eq. C.1 is sometimes altered i the actual production process because particles are non-spherical or agglomerated.

To test the validity of Eq. C.1, the relative specific activity (% activity/% mass) for the sieve fractions of each batch has been plotted (log-log scale) against the reciprocal 1/d (computed from sieve fraction mid-size, μ). The resultant curves are shown in Figs. C.1 and C.2. For these logarithmic plots to obey Eq. C.1, the curves should all be straight parallel lines having a slope of unity. At first the curves do not appear to satisfy these conditions, but when Tables C.1 through C.6 are reviewed the situation improves. The bulk of the mass and activity of each batch sample is contained in three or four sieve fractions corresponding to the control percentages mentioned earlier. The remainder in two cases is less than 15 % of the total mass and activity, and in three cases is less than 10 %. The solid data points in Figs. C.1 and C.2 represent these control percentages. Straight-line curves have been fitted to these controlling points, and they meet the conditions dictated by Eq. C.1.

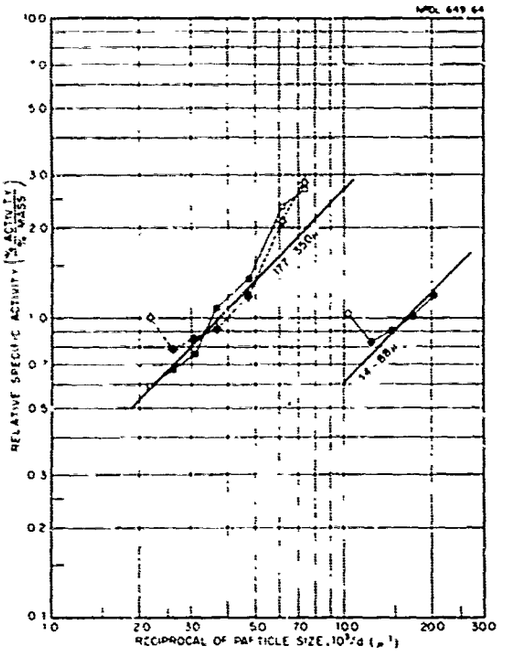

Fig. C.1 Approximate Fit of Eq. C.1 to Simulant Activity/Size Data - Particle Size Ranges A and C.

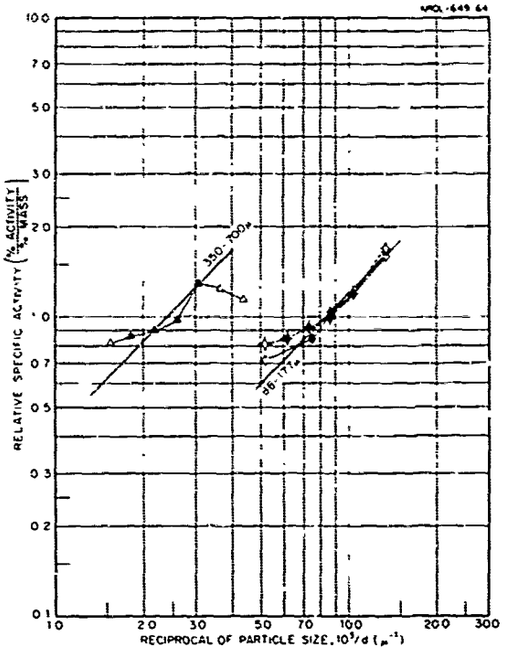

Fig. C.2 Approximate Fit of Eq. C.1 to Simulant Activity/Size Data - Particle Size Ranges B and D.

APPENDIX D

RADIATION DATA

D.1 SHIELDED DETECTOR DATA

Table D.1 presents the reduced radiation data from the shielded gamma detector for the fire nozzle tests. The second column, nominal mass loading (M_o), shows the proposed weight to be spread for that test. The average initial radiation ($\bar{I}_o$) is the radiation level from the actual mass dispersed. The average residual radiation ($\bar{I}$) is the level of radiation remaining after each firehosing pass. The average fraction remaining ($\bar{F}$) is the ratio $\bar{I}/\bar{I}_o$.

D.2 REDUCED RADIAC (PDR-27C) DATA

Table D.2 presents the average values reduced from the radiac data for the flare nozzle tests. This table contains the same type of information as Table D.1 except that the radiation values are in mr/hr instead of counts per minute (cpm).

D.3 ORIGINAL FIRE NOZZLE DATA

The data compiled in Table D.3 were averaged from two raw counts of one-minute duration at 18 stations and reduced as follows:

TABLE D.1

Reduced Shielded Detector Data - Fire Nozzle Only

Test No.	Nominal Mass Loading (g/ft^2)	Average Initial Radiation, $\bar{I}_o$ (cpm)	Pass No.	Average Residual Radiation, $\bar{I}$ (cpm)	Average Fraction Remaining, $\bar{F}$
		PSR: A, 44-88 μ			
A-1	4.0	397,599	1	82,087	0.206
			2	61,805	0.155
A-2	4.0	481,757	1	107,005	0.222
			2	77,903	0.162
			3	69,652	0.145
A-3	24.0	2,549,671	1	216,279	0.085
			2	164,364	0.064
A-4	24.0	2,435,211	1	791,914	0.325
			2	681,842	0.280
			3	621,978	0.255
			4	607,851	0.250
		PSR: B, 88-177 μ			
B-1	4.0	120,259	1	20,310	0.169
			2	12,790	0.106
B-2	4.0	133,130	1	85,935	0.645
			2	58,573	0.440
			3	38,493	0.289
			4	29,636	0.223
B-3	50.0	2,058,316	1	90,715	0.044
			2	82,401	0.040
B-4	50.0	2,043,342	1	358,323	0.175
			2	116,318	0.057
			3	79,008	0.039
			4	66,285	0.032

Continued

TABLE D.1 (Cont'd)

Reduced Shielded Detector Data - Fire Nozzle Only

Test No.	Nominal Mass Loading (g/ft^2)	Average Initial Radiation $\bar{I}_o$ (cpm)	Pass No.	Average Residual Radiation $\bar{I}$ (cpm)	Average Fraction Remaining $\bar{F}$
		PSR: B, 88-177 μ			
B-6	24.0	1,755,379	1	39,747	0.023
			2	25,123	0.014
B-7	24.0	1,916,568	1	372,784	0.194
			2	97,558	0.051
			3	66,784	0.035
			4	59,556	0.031
B-8	100.0	7,446,790	1	92,759	0.012
			2	11,580	0.001
B-9	100.0	7,101,193	1	1,753,509	0.247
			2	293,116	0.041
			3	154,242	0.022
			4	114,956	0.016
		PSR: C, 177-350 μ			
C-1	4.0	528,272	1	24,592	0.046
			2	12,778	0.024
C-2	12.0	1,561,838	1	60,213	0.038
			2	17,184	0.011
C-3	24.0	2,553,655	1	34,551	0.013
			2	13,062	0.005
C-4	50.0	5,161,797	1	29,417	0.0057
			2	14,954	0.0029
C-6	4.0	554,878	1	87,723	0.158
			2	51,081	0.092
			3	16,860	0.030
			4	11,088	0.020

Continued

TABLE D.1 (Cont'd)

Reduced Shielded Detector Data - Fire Nozzle Only

Test No.	Nominal Mass Loading (g/ft^2)	Average Initial Radiation $\overline{I_o}$ (cpm)	Pass No.	Average Residual Radiation $\overline{I}$ (cpm)	Average Fraction Remaining $\overline{F}$
		PSR: C, 177-350 μ			
C-7	12.0	1,032,502	1	169,688	0.164
			2	69,030	0.067
			3	33,082	0.032
			4	22,983	0.022
C-8	24.0	2,398,132	1	333,700	0.139
			2	51,695	0.021
			3	27,353	0.011
			4	17,617	0.007
C-9	50.0	5,185,923	1	1,173,700	0.225
			2	82,958	0.016
			3	33,483	0.006
			4	27,152	0.005
		PSR: D, 350-700 μ			
D-1	4.0	363,750	1	3,257	0.0089
			2	2,062	0.0057
D-2	4.0	451,922	1	70,288	0.1555
			2	15,846	0.0351
			3	7,795	0.0172
D-3	24.0	2,020,250	1	22,851	0.0113
			2	7,085	0.0035
D-4	24.0	1,939,914	1	245,964	0.1268
			2	34,536	0.0178

TABLE D.2

Reduced Radiac Data - Flare Nozzle Only

Test No.	Particle Size Range, PSR (μ)	Nominal Mass Loading (g/ft^2)	Average Initial Radiation, $\bar{I}_o$ (mr/hr)	Pass No.	Average Residual Radiation, $\bar{I}$ (mr/hr)	Average Fraction Remaining, $\bar{F}$
A-5	44-88	24.0	199.4	1	3.3	0.016
				2	0.8	0.004
B-5	88-177	24.0	51.7	1	2.2	0.042
				2	0.4	0.008
C-5	177-350	24.0	227.9	1	3.5	0.015
				2	2.8	0.012
C-10	177-350	24.0	196.1	1	0.5	0.0025
				2	0.3	0.0015
D-5	350-700	24.0	201.8	1	3.0	0.0149
				2	1.7	0.0084

TABLE D.3

Typical Sample of Original Data in CPM From Shielded γ Detector Fire Nozzle Only

Station	Background	Initial I_o	1st Pass I_1	2nd Pass I_2
Test No. C-3 Date: 9/19/63				
1	1,314	917,449	3,179	2,567
2		864,424	5,107	4,503
3	3,671	877,589	55,584	11,325
4		920,627	18,607	3,938
5	2,792	936,666	7,717	9,449
6		988,754	9,501	9,646
7	2,547	897,614	8,766	5,973
8		972,317	4,131	3,778
9	3,141	942,940	14,050	8,893
$\bar{I}$	2,693	924,264	14,071	6,675
$\bar{I}_c$	0	2,834,659	36,418	13,896
11	3,921	713,458	9,089	6,033
12		758,918	15,769	7,059
13	1,644	765,851	40,010	5,420
14		752,167	4,465	7,973
15	2,388	688,823	8,049	5,610
16		712,900	4,712	8,638
17	1,381	709,337	9,600	2,816
18		741,104	12,677	4,278
19	2,038	724,898	7,444	2,872
$\bar{I}$	2,274	729,723	12,424	5,633
$\bar{I}_c$	0	2,272,652	33,033	12,229

Starting with the average radiation count $\bar{I}$, the corrected zero time count $\bar{I}_c$ may be derived from the equation:

$$\bar{I}_c = \frac{\bar{I}\,(\text{Standard Factor}) - \text{Adjusted Background}}{\text{Decay Factor}} \qquad \text{(D.1)}$$

from a standard cobalt source. Thus

$$\text{Standard Factor} = \frac{100{,}000 \text{ cpm}}{\text{Avg } Co^{60} \text{ cpm}} \qquad \text{(D.2)}$$

where 100,000 cpm is an arbitrary value approximately equal to the daily average standard count. The denominator is the average of standard counts taken just before and just after obtaining the survey values comprising $\bar{I}$. The standard factor serves the purpose of compensating for fluctuations in instrument response by normalizing original counts to a common reference.

The decay factor simply corrects for the decay effects of the La^{140} tracer. It is based on a 40.2-hr half-life and is calculated for the time interval from zero time to the mid-time of a given test run. Zero time is 1200 hours on Monday of the week in which the simulant was produced.

The background count is made up of two values. First, there is the residual calculated background caused by residual La^{140} contamination from previous tests. Second, there is the natural background which is relatively small and is ignored except in the very first test. The residual background count is adjusted for the effects of instrument response and isotope decay in the same manner as described above for $\bar{I}$. Natural background requires no zero time correction since it is a constant value.

D.4 RAW FLARE NOZZLE DATA

Table D.4 readings in mr/hr at nine stations were averaged and reduced as follows:

Starting with the average radiation value $\bar{I}$, the corrected zero time value $\bar{I}_c$ may be derived from the equation:

$$\bar{I}_c = \frac{\bar{I} - \text{Adjusted Background}}{\text{Decay Factor}} \qquad (D.3)$$

The radiacs were frequently checked with a Co^{60} standard to eliminate errors due to faulty electronics or shifts in calibration.

TABLE D.4

Original Data in mr/hr From Radiac Instrument - Flare Nozzle Only

Station	Background	Initial I_o	1st Pass I_1	2nd Pass I_2
Test No. A-5 Date: 10/14/63				
1	3.7	11.0	3.3	3.5
2	4.4	14.0	4.5	4.3
3	4.5	15.0	4.7	4.4
4	4.7	14.0	4.8	4.6
5	4.4	16.0	4.8	4.7
6	4.5	16.0	4.8	4.6
7	4.5	20.0	4.7	4.3
8	4.3	18.0	4.5	4.4
9	4.3	17.0	4.3	4.3
$\bar{I}$	4.4	15.7	4.5	4.3
$\bar{I}_c$	75.3	199.6	3.4	0.8
Test No. B-5 Date: 10/21/63				
1	0.9	3.9	1.2	1.1
2	1.2	4.3	1.3	1.3
3	1.3	4.3	1.4	1.4
4	1.3	4.3	1.4	1.3
5	1.4	4.4	1.6	1.4
6	1.4	4.3	1.5	1.4
7	1.3	4.4	1.6	1.4
8	1.3	4.6	1.4	1.4
9	1.2	4.3	1.3	1.3
$\bar{I}$	1.3	4.3	1.4	1.3
$\bar{I}_c$	21.7	52.6	3.0	1.6
Test No. C-5 Date: 10/28/63				
1	0.3	12.0	0.4	0.4
2	0.4	14.0	0.5	0.5
3	0.4	14.0	0.6	0.5
4	0.4	13.0	0.6	0.5
5	0.4	14.0	0.6	0.6
6	0.5	15.0	0.7	0.6
7	0.4	14.0	0.7	0.6
8	0.4	13.0	0.6	0.7
9	0.5	12.0	0.7	0.7
$\bar{I}$	0.4	13.4	0.6	0.6
$\bar{I}_c$	7.2	228.6	3.5	3.0

Continued

TABLE D.4 (Cont'd)

Original Data in mr/hr From Radiac Instrument - Flare Nozzle Only

Station	Background	Initial I_o	1st Pass I_1	2nd Pass I_2
Test No. C-10 Date: 10/29/63				
1	0.2	7.0	0.3	0.3
2	0.3	8.0	0.3	0.3
3	0.3	8.0	0.3	0.3
4	0.3	8.0	0.4	0.3
5	0.4	8.0	0.4	0.4
6	0.4	8.0	0.4	0.4
7	0.4	8.0	0.4	0.4
8	0.4	8.0	0.4	0.4
9	0.4	7.0	0.4	0.4
$\bar{I}$	0.3	7.8	0.4	0.4
$\bar{I}_c$	9.1	195.6	0.7	0.4
Test No. D-5 Date: 11/1/63				
1	0.1	8.0	0.2	0.2
2	0.1	9.0	0.2	0.2
3	0.1	8.0	0.2	0.2
4	0.1	8.0	0.2	0.2
5	0.1	8.0	0.2	0.2
6	0.1	8.0	0.2	0.2
7	0.1	7.0	0.2	0.2
8	0.1	8.0	0.3	0.2
9	0.1	8.0	0.3	0.2
$\bar{I}$	0.1	8.0	0.2	0.2
$\bar{I}_c$	3.3	201.8	3.0	1.7

SUMMARY OF RESEARCH REPORT

REMOVAL OF SIMULATED FALLOUT FROM ASPHALT STREETS BY FIREHOSING TECHNIQUES

USNRDL-TR-1049

by L. L. Wiltshire, W. L. Owen

PURPOSE AND OBJECTIVES

Firehosing has held the interest of investigators in the field of radiological recovery for many years, because of its broad application and ready availability. Related reclamation studies have shown firehosing to be an especially effective fallout removal method. Interpretation of test results, however, was limited largely to demonstrating the dependence of removal effectiveness upon fallout mass loading and firehosing effort, without regard to the effects of fallout particle size range. Since the last firehosing experiments (Stoneman II, 1958), facilities had been developed at the USNRDL Station at Camp Parks to produce simulant in five distinct particle size ranges. Subsequent tests there of other methods, sweeping and street flushing, showed removal effectiveness to be a function of particle size range. Therefore it became necessary to investigate this effect on firehosing performance.

The purpose of this experiment was to establish optimum firehosing performance characteristics by observing the interaction between removal effectiveness and those factors affecting operational efficiency.

The objectives in support of the above were as follows:

1. To determine and measure equipment variables governing firehosing performance.

2. To establish (within practical manpower limits) the most effective firehosing technique.

3. Under the optimum combination of operational variables found in 1 and 2 above, to measure firehosing performance in terms of removal effectiveness and required effort.

All three objectives were investigated for a limited selection of fallout mass loadings and particle size ranges.

SCOPE

The experiment was performed in two major stages, preliminary and principal. The preliminary stage involved 19 tests conducted with inert (non-radioactive) sand simulant. These tests met the first two objectives by resolving such operational factors as stream range* and hosing technique. The principal stage consisted of 29 tests performed with radio-traced simulant. These tests met the third objective by

* Stream range is the distance between the nozzle and the point of stream impact.

determining the effects of cleaning rate, particle size, mass loading, and stream pattern* on firehosing effectiveness.

Of the 29 principal tests, 24 employed a conventional 5/8-in. orifice fire nozzle. Two tests were conducted for each of 12 simulated fallout conditions. For each pair of tests, the first progressed at a slow (visually controlled**) firehosing rate, and the second was performed at approximately twice the visual rate. The remaining five tests employed an NRDL experimental "flare" nozzle and were run at the visual rate only. All tests were conducted on the same asphalt surface.

The 12 simulated radiological conditions were defined by particle size ranges of 44-88 μ, 88-177 μ, 177-350 μ, and 350-700 μ; and by mass loadings of 4, 12, 24, 50 and 100 g/ft^2. The mass loading selections were predicted from C. F. Miller's fallout model which also completely described such radiological conditions as weapon yield, standard intensity and down wind distance.

FINDINGS

The preliminary firehosing tests determined that:

1. The most effective firehosing technique tested was frontal sweeping. In this technique the fire hose stream pushed the material down slope toward a collecting point (catch basin) located at the curb.

2. For a given fire nozzle and pressure, optimum stream range is dependent upon particle size.

3. For the 5/8-in. orifice fire nozzle operating at 75 psi, the optimum stream range (for all practical purposes) is greater than 15 ft. and not more than 30 ft.

CONCLUSIONS

From the principal tests, the following conclusions can be made:

1. In studying the effect of firehosing rate on specific mass loadings in all particle size ranges it is apparent that:

a. In most cases, the slow (visually controlled) rate of firehosing will remove more material than the fast rate for the same amount of effort. Doubling the visual rate generally increases the residual mass by a factor of 2 or more.

* Stream pattern is the shape of the water stream leaving the nozzle.
**The rate at which the fallout is seen to be moved ahead by the water stream.

b. Firehosing teams can operate at the slow rate for longer periods of time before tiring.

2. In general, removal effectiveness of firehosing improves with increased particle size range and increased mass loading.

For the expenditure of an effort of 4 nozzle-minutes (12 man-minutes) per 10^3 ft^2, results ranged as follows:

Particle Size Range (μ)	Nominal Mass Loading (g/ft^2)	Removal Effectiveness (Residual Fraction)
44 - 88	4.0	0.16
	24.0	0.07
350 - 700	4.0	0.005
	24.0	0.003

3. The effects of stream pattern were not completely established. It is quite possible that hosing performance can be improved through use of the flare nozzle, if the nozzle pressure is kept at 150 psi or greater.

4. The previously developed empirical cleaning formula ($M = M^* + (M_0 - M^*) \exp. -3 K E^{1/3}$) is more adaptable to data obtained from flare nozzle tests.

RECOMMENDATIONS

These firehosing studies should be extended to include the following:

1. Mount a full-scale test based on these engineering test results which will produce a dose rate history of the recovery team that would allow derivation of RN_2 factors (recovery crew exposure reduction factors).

2. Investigate the promising performance of the flare nozzle on paved areas.

3. Compare the performance of the 5/8-in. fire nozzle and the flare nozzle on common roofing materials.

The above studies should include observance of the effects of mass loading and particle size range.

UNCLASSIFIED
Security Classification

DOCUMENT CONTROL DATA - R&D

(Security classification of title, body of abstract and indexing annotation must be entered when the overall report is classified)

1. ORIGINATING ACTIVITY (Corporate author)	2a. REPORT SECURITY CLASSIFICATION
U. S. Naval Radiological Defense Laboratory San Francisco, California 94135	UNCLASSIFIED 2b GROUP

3. REPORT TITLE

REMOVAL OF SIMULATED FALLOUT FROM ASPHALT STREETS BY FIREHOSING TECHNIQUES

4. DESCRIPTIVE NOTES (Type of report and inclusive dates)

5. AUTHOR(S) (Last name, first name, initial)

Wiltshire, Lyman L.
Owen, W. Leigh

6. REPORT DATE	7a. TOTAL NO. OF PAGES	7b. NO. OF REFS
7 November 1966	103	7

8a. CONTRACT OR GRANT NO.	9a. ORIGINATOR'S REPORT NUMBER(S)
b. PROJECT NO.	USNRDL-TR-1049
c. OCD-TO-65-200(22), Work Unit 3212A	9b. OTHER REPORT NO(S) (Any other numbers that may be assigned this report)
d.	

10. AVAILABILITY/LIMITATION NOTICES

Distribution of this document is unlimited.

11. SUPPLEMENTARY NOTES	12. SPONSORING MILITARY ACTIVITY
	Office of Civil Defense Washington, D.C. 20310

13. ABSTRACT

This report evaluates firehosing as a wet reclamation procedure for the operational recovery of asphalt paved streets contaminated with fallout from a land surface nuclear detonation. Preliminary tests with inert fallout simulant determined the optimum nozzle stream range and firehosing technique. Principal tests, conducted with radio-traced simulants, measured the effects of hosing rate, stream pattern, particle size and mass loading on the fallout removal performance of firehosing.

Several conclusions were indicated: (1) A slow hosing rate (visually controlled) was more effective than a faster rate, regardless of mass loading or particle size range. (2) The removal effectiveness improved with increased particle size range and increased mass loading. (3) An experimental NRDL "flare" nozzle appeared to improve hosing performance at nozzle pressures greater than 150 psi.

Graphs showing the effect of hosing rate, particle size, mass loading and stream pattern on the reclamation performance of firehosing are presented.

DD FORM 1 JAN 64 1473

UNCLASSIFIED
Security Classification

UNCLASSIFIED
Security Classification

14 KEY WORDS	LINK A		LINK B		LINK C	
	ROLE	WT	ROLE	WT	ROLE	WT
Performance curves Stream range effects Hosing rate effects Particle size effects Mass loading effects Stream pattern effects Hosing theory						

INSTRUCTIONS

1. ORIGINATING ACTIVITY: Enter the name and address of the contractor, subcontractor, grantee, Department of Defense activity or other organization *(corporate author)* issuing the report.

2a. REPORT SECURITY CLASSIFICATION: Enter the overall security classification of the report. Indicate whether "Restricted Data" is included. Marking is to be in accordance with appropriate security regulations.

2b. GROUP: Automatic downgrading is specified in DoD Directive 5200.10 and Armed Forces Industrial Manual. Enter the group number. Also, when applicable, show that optional markings have been used for Group 3 and Group 4 as authorized.

3. REPORT TITLE: Enter the complete report title in all capital letters. Titles in all cases should be unclassified. If a meaningful title cannot be selected without classification, show title classification in all capitals in parenthesis immediately following the title.

4. DESCRIPTIVE NOTES: If appropriate, enter the type of report, e.g., interim, progress, summary, annual, or final. Give the inclusive dates when a specific reporting period is covered.

5. AUTHOR(S): Enter the name(s) of author(s) as shown on or in the report. Enter last name, first name, middle initial. If military, show rank and branch of service. The name of the principal author is an absolute minimum requirement.

6. REPORT DATE: Enter the date of the report as day, month, year; or month, year. If more than one date appears on the report, use date of publication.

7a. TOTAL NUMBER OF PAGES: The total page count should follow normal pagination procedures, i.e., enter the number of pages containing information.

7b. NUMBER OF REFERENCES: Enter the total number of references cited in the report.

8a. CONTRACT OR GRANT NUMBER: If appropriate, enter the applicable number of the contract or grant under which the report was written.

8b, 8c, & 8d. PROJECT NUMBER: Enter the appropriate military department identification, such as project number, subproject number, system numbers, task number, etc.

9a. ORIGINATOR'S REPORT NUMBER(S): Enter the official report number by which the document will be identified and controlled by the originating activity. This number must be unique to this report.

9b. OTHER REPORT NUMBER(S): If the report has been assigned any other report numbers *(either by the originator or by the sponsor)*, also enter this number(s).

10. AVAILABILITY/LIMITATION NOTICES: Enter any limitations on further dissemination of the report, other than those imposed by security classification, using standard statements such as:

(1) "Qualified requesters may obtain copies of this report from DDC."

(2) "Foreign announcement and dissemination of this report by DDC is not authorized."

(3) "U. S. Government agencies may obtain copies of this report directly from DDC. Other qualified DDC users shall request through _____."

(4) "U. S. military agencies may obtain copies of this report directly from DDC. Other qualified users shall request through _____."

(5) "All distribution of this report is controlled. Qualified DDC users shall request through _____."

If the report has been furnished to the Office of Technical Services, Department of Commerce, for sale to the public, indicate this fact and enter the price, if known.

11. SUPPLEMENTARY NOTES: Use for additional explanatory notes.

12. SPONSORING MILITARY ACTIVITY: Enter the name of the departmental project office or laboratory sponsoring *(paying for)* the research and development. Include address.

13. ABSTRACT: Enter an abstract giving a brief and factual summary of the document indicative of the report, even though it may also appear elsewhere in the body of the technical report. If additional space is required, a continuation sheet shall be attached.

It is highly desirable that the abstract of classified reports be unclassified. Each paragraph of the abstract shall end with an indication of the military security classification of the information in the paragraph, represented as *(TS), (S), (C), or (U)*.

There is no limitation on the length of the abstract. However, the suggested length is from 150 to 225 words.

14. KEY WORDS: Key words are technically meaningful terms or short phrases that characterize a report and may be used as index entries for cataloging the report. Key words must be selected so that no security classification is required. Identifiers, such as equipment model designation, trade name, military project code name, geographic location, may be used as key words but will be followed by an indication of technical context. The assignment of links, roles, and weights is optional.